united nations
educational, scientific
and cultural
organization

international atomic
energy agency

the
**abdus salam**
international centre for theoretical physics

ICTP 40th Anniversary

*SCHOOL ON SYNCHROTRON RADIATION AND APPLICATIONS*
*In memory of J.C. Fuggle & L. Fonda*

**19 April - 21 May 2004**

*Miramare - Trieste, Italy*

**1561/36**

---

# Photo emission electron microscopy - Outline

**E. Bauer**

# Photo emission electron microscopy

## Outline

**Introduction**

**Electron optics**
- **Resolution**
- **Transmission**

**Instruments**
- **PEEM**
- **PEEM + LEEM**

**Methodic**

**Application examples**
- **Chemical imaging**
- **Magnetic imaging**

# Photo Emission Electron Microscopy (PEEM)

**2 types**

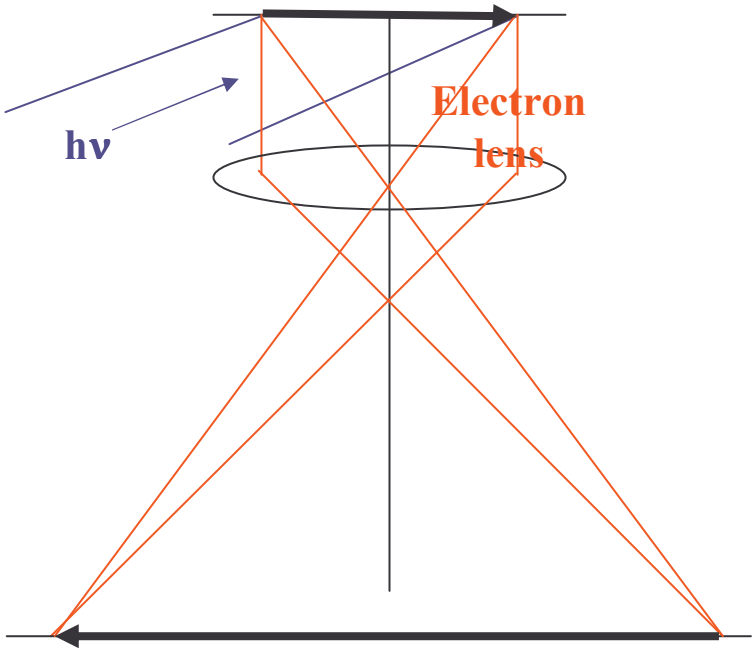


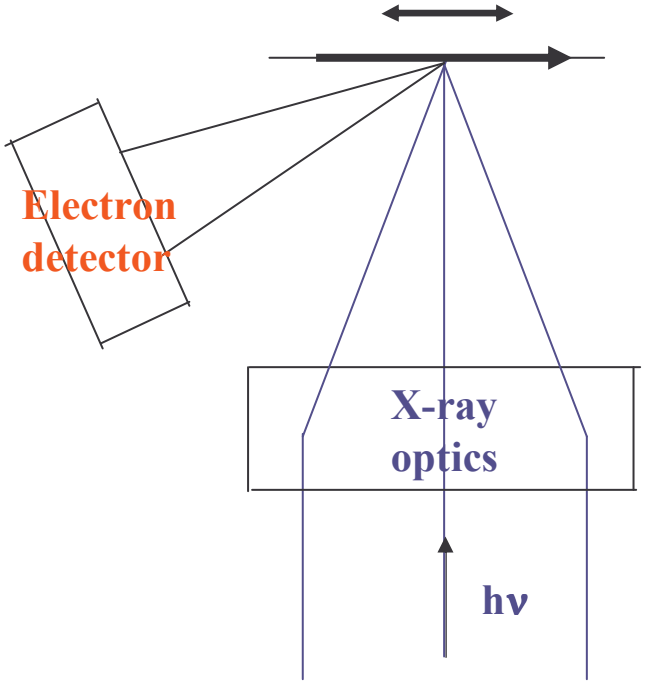


**broad illumination** | **focused illumination**

**Full field** | **PEEM** | **Scanning**

**sample fixed** | **sample scanned**

**Bauer** | **Kiskinova**

# 4 imaging modes

| | | | |
|---|---|---|---|
| 1 | Threshold UV- and X-PEEM | Photoelectrons PE | with |
| 2 | XPEEM | “ | energy |
| 3 | XAEEM | Auger electrons AE | filter |
| 4 | XSEEM | Secondary electrons SE | |

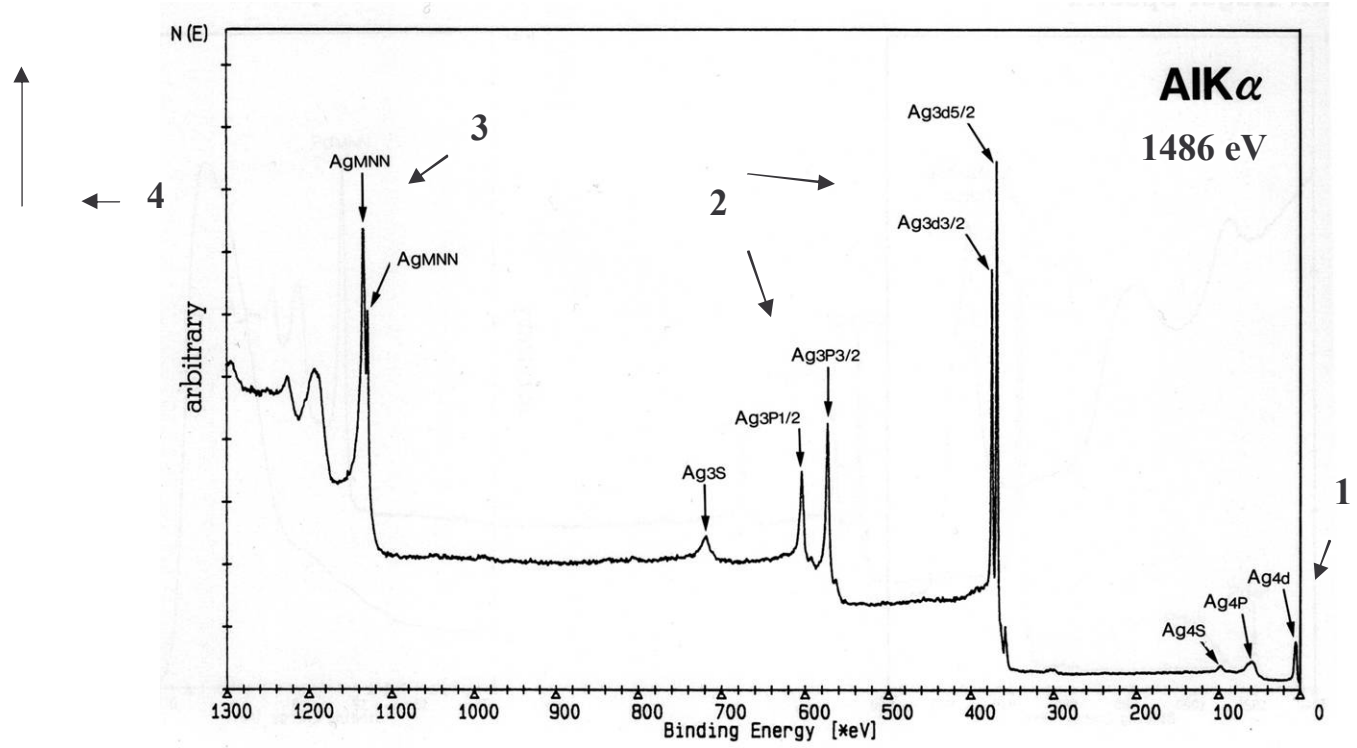

# Angular distribution

## Internal

**Amorphous, polycrystalline, SE**

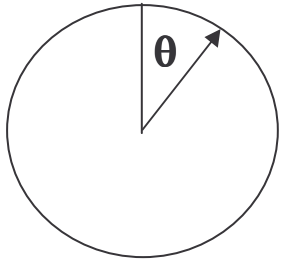


$I_i(\theta)$ = const.

**single crystalline, PE, AE**

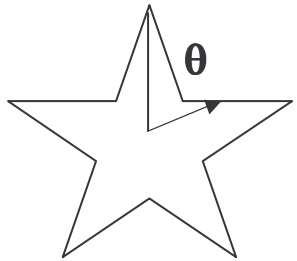


$I_i(\theta)$ due to diffraction

## Internal (i) → External (e)

n ~ √E

√(E+V₀)

**Refraction**

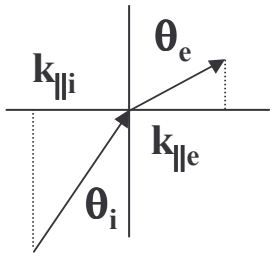


**$k_{||}$ conservation** $k_{||e} = k_{||i}$

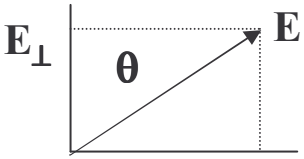


$E_\perp = E \cos\theta$

**For escape necessary:**

$E_\perp > \Phi$ (work function)

I (ionization energy)

U (HOMO)

## External

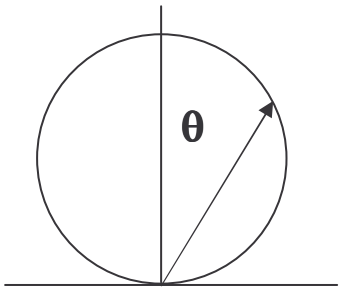


$I_e(\theta) = \cos\theta$

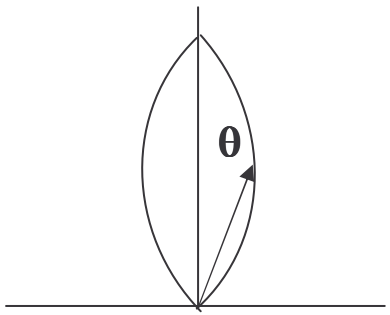

# Electron optics

# The cathode lens

In emission microscopy θ is large
Electron lenses can accept only small θ because of large chromatic and spherical aberrations
Solution of problem: accelerate electrons to high energy before lens →

Immersion objective lens = cathode lens

$$n \sin\theta = \text{const}$$
$$n \sim v \sim \sqrt{E}$$
$$\theta \rightarrow \alpha$$
$$\sin\alpha / \sin\alpha_0 = \sqrt{E_0/E}$$

Example for E = 20000 eV:

| $E_0$ | 2 eV | 200 eV |
|---|---|---|
| $\alpha$ for $\alpha_0 = 45^o$ | $0.4^o$ | $4.5^o$ |

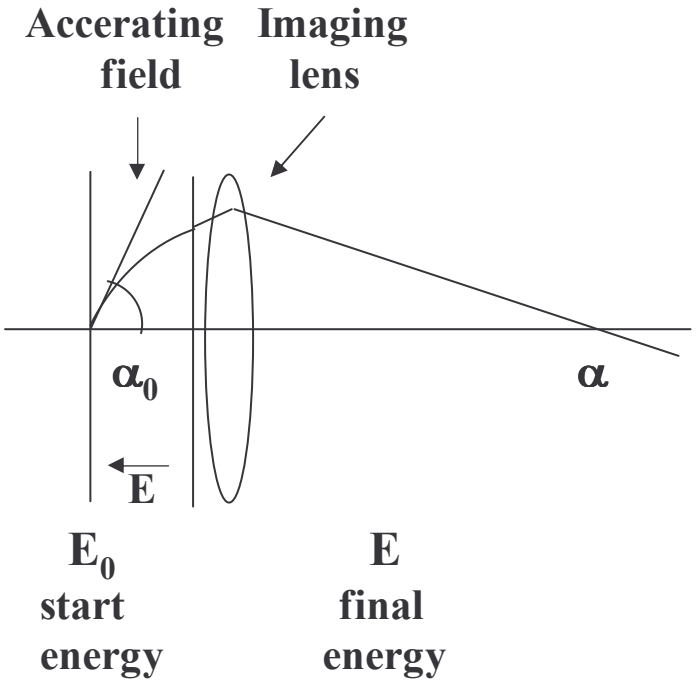

# Cathode lens types

## Electrostatic tetrode

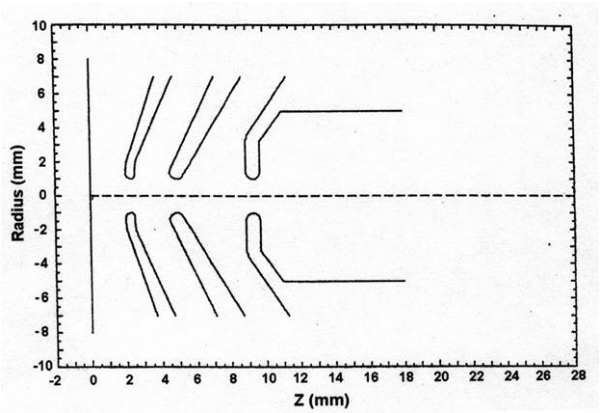


## Lens comparison

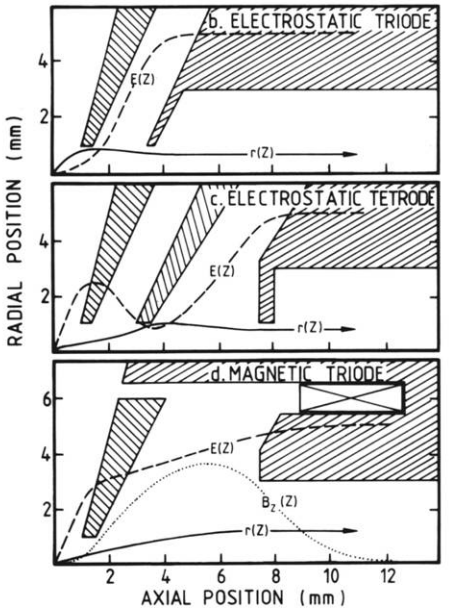


**Estimation of aberrations:**
**Separate lens into acceleration and imaging regions**

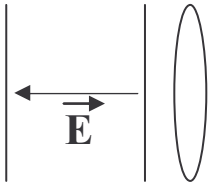


**At low energies aberrations of accelerating region dominates**

# Aberrations

## chromatic

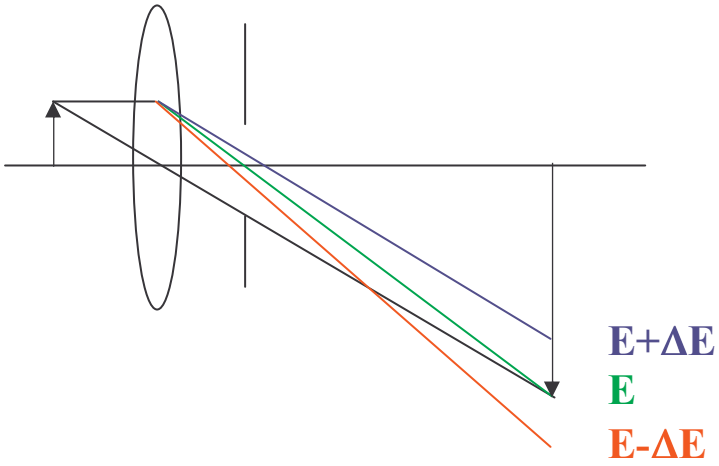


slower (faster) electrons
are more (less) deflected

## spherical

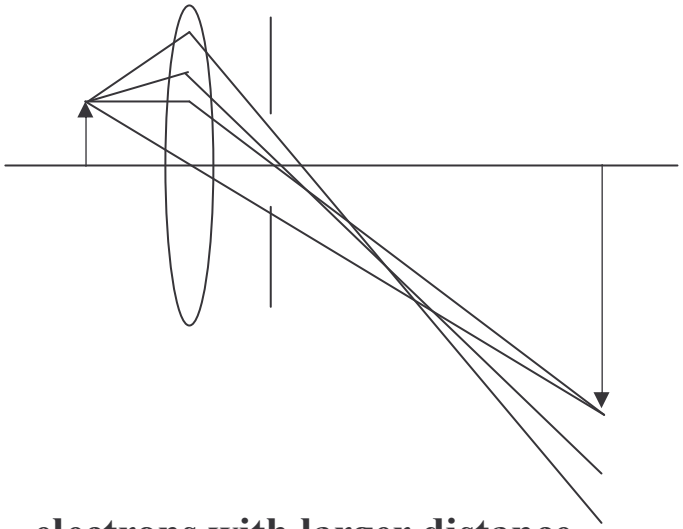

electrons with larger distance
from axis are more deflected
(stronger field!)

# Aberrations of homogeneous acceleration field

$\rho_0 = E_0/E \qquad \varepsilon = \Delta E_0/E \qquad \rho = \rho_0 + \varepsilon$

**Spherical aberration $D_{ö}$**

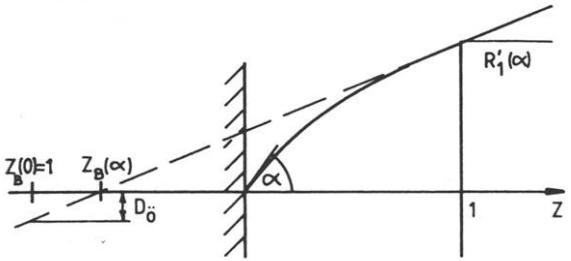


**Chromatic aberration $D_F$**

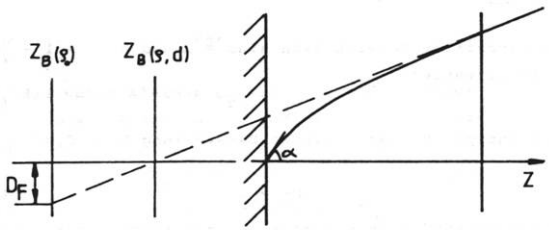


**Approximation: $\rho_0$ and $\varepsilon \ll 1/\cos\alpha^2 > 1$**
**Example: $E_0 = 100$ eV, $\Delta E_0 = 1$ eV, $E = 20000$ eV**
**$\varepsilon = \rho_0 /100$, $\rho_0 = 1/200$**

$D_{ö} \approx 2\,\rho \sin\alpha\,(1 - \cos\alpha)$

$\approx \rho\,\alpha^3$ for small $\alpha$

$D_F \approx 2\,\rho \sin\alpha\,(\sqrt{\rho_0 / \rho} - 1)$

$\approx \varepsilon \sin\alpha$ for $\varepsilon \ll \rho_0$

$\approx \varepsilon\,\alpha$ for small $\alpha$

**α-dependent aberrations require α-limitation by angle-limiting aperture ("contrast aperture") with radius $r_A$**

↓

**Diffraction by aperture: diffraction disc of confusion $d_B = 0.6\,\lambda / r_A$**

**Approximate resolution $d = \sqrt{d_ö^2 + d_F^2 + d_B^2}$**

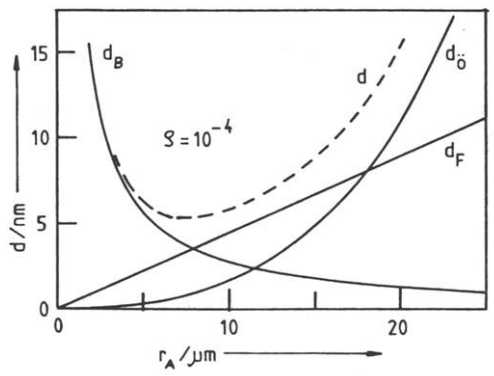


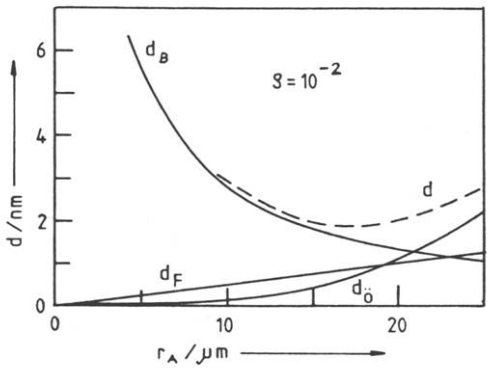


**L = 3 mm  E = 25000 eV  $\Delta E_0$ = 0.25 eV**

**Optimum aperture radius**

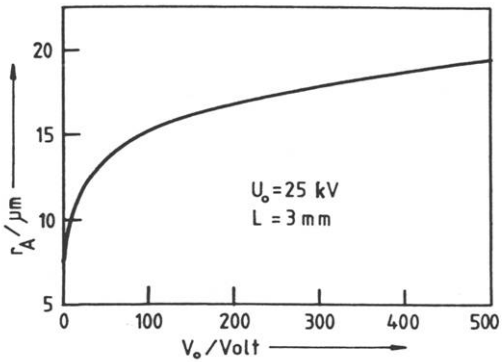


**Optimum resolution**

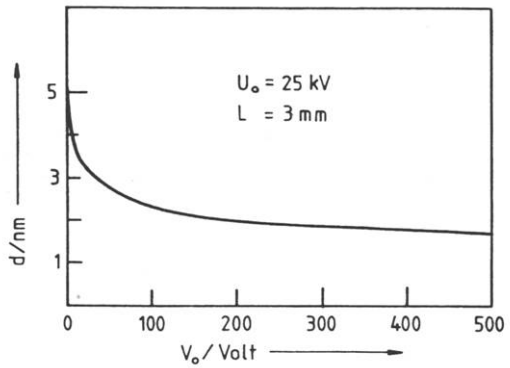


**Note: small angle approximation $\sin\alpha \approx \alpha \sim r$**

# Transmission

## limited by angle accepted by contrast aperture ($r_A$)

Axial distance (in back focal plane) of electron starting at angle $\alpha$

$r \approx f \sin\alpha \sqrt{E_0/E}$ (f focal length)_

$$\sin\alpha \approx (r/f)\sqrt{E_0/E}$$

Examples for f = 10 mm, E = 20000eV, $r_A$ =10 μm

| $E_0$ | 2 eV | 200 eV |
|---|---|---|
| $\sin\alpha$ | 0.2 | 0.02 |
| $\alpha$ | 11.5° | 1.15° |

In emission microscopy (wide $\alpha$ range) optimum resolution condition reduces transmission T, therefore

optimize $T^n/d^2$ instead of $1/d^2$

For cos $\alpha$ distribution $T = \pi \sin^2\alpha$

$$T^n/d^2 = \pi \sin^{2n}/d^2$$

# Transmission $T_n$, resolution $r_n$ of homogeneous field

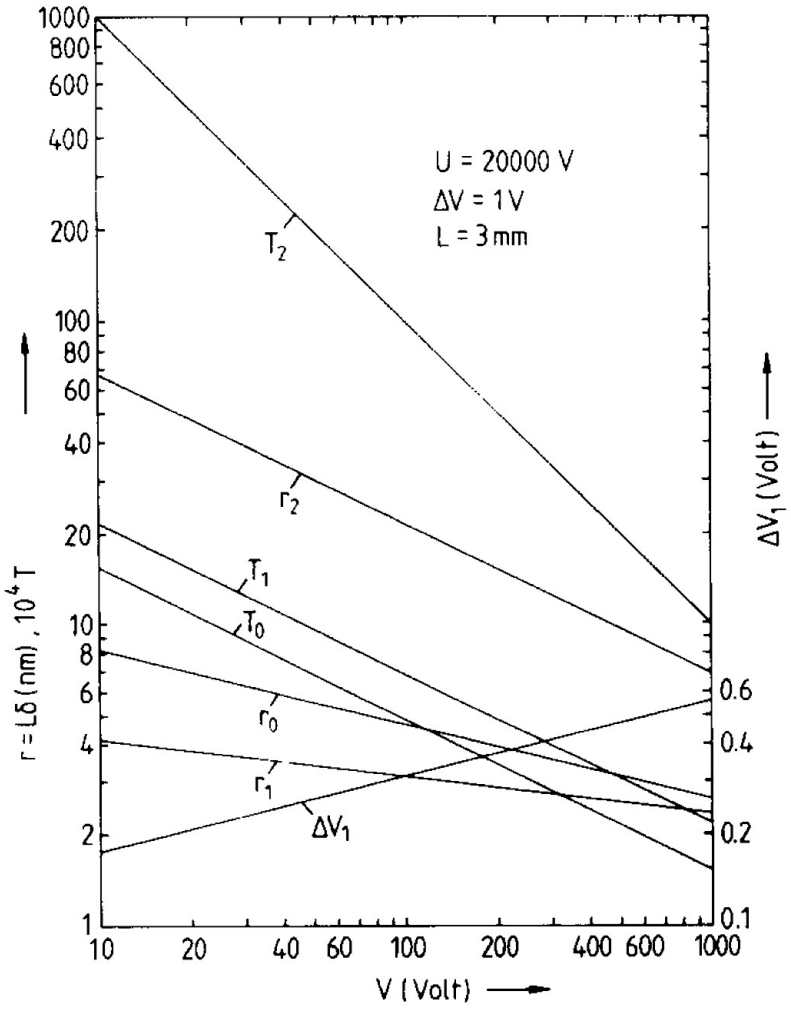


E. Bauer, Ultramicroscopy 36 (1991) 52

# Influence of angle-limiting aperture on the energy distribution of secondary electrons

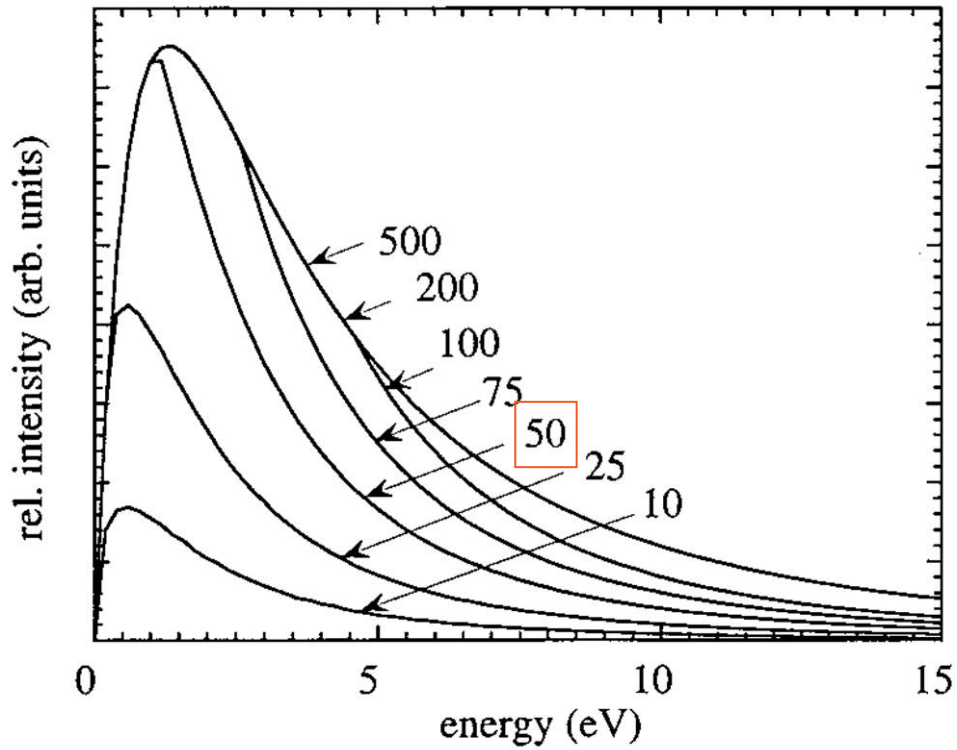


**Work function Φ = 4 eV, accelerating voltage V = 20 kV**
**Parameter: aperture diameter in µm, ALS PEEM**

S. Anders et al, Rev. Sci. Instrum. 70 (1999) 3973

# Real lenses

## Acceleration and imaging fields combined
## Electrostatic triode

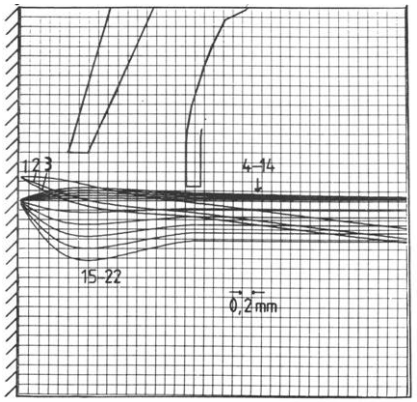


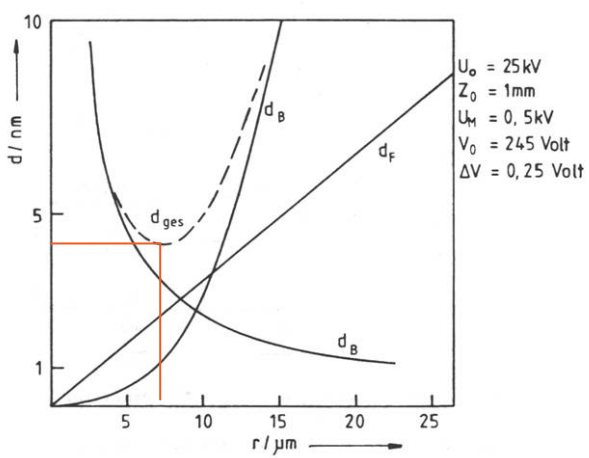


**Optimum aperture**

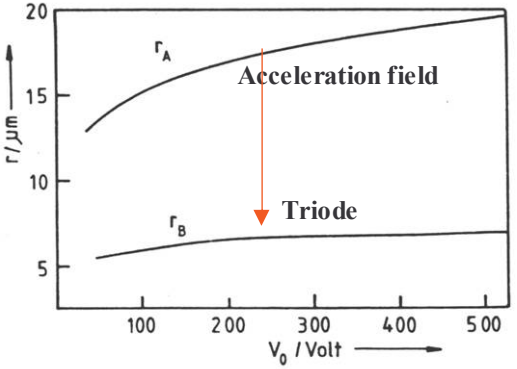


1,3: $z_F$, f, $z_I$
1,2 (ΔE): $c_c$
15-22 (×50): $c_s$ $\alpha_{max} = 9^o$
4-14 to scale $\alpha_{max} = 80^o$

**Resolution**

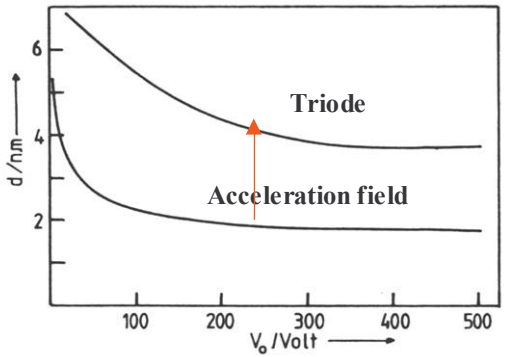


D.R. Cruise, J. Appl. Phys. 35 (1964) 3080

# Resolution and optimum aperture

**Optimum aperture r and resolution-limiting contributions**

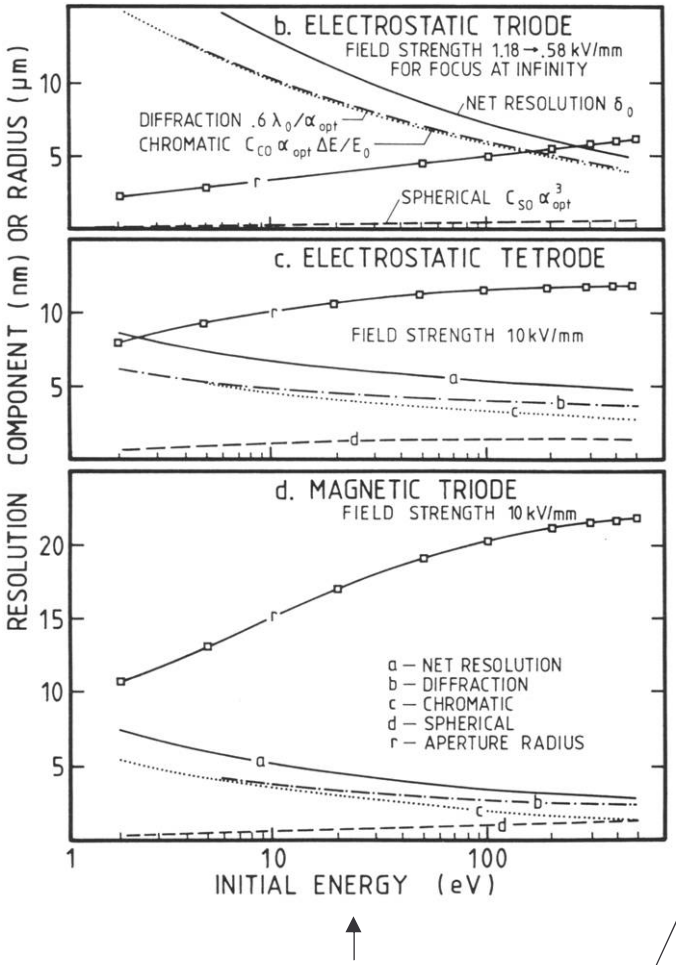


J. Chmelik et al, Optik 83 (1989)155

T. Müller, M.S. thesis, TU Clausthal 1995

**Resolution with optimum aperture**
**E-dependence at fixed ΔE = 0.5 eV, $U_0$ = 20 keV**

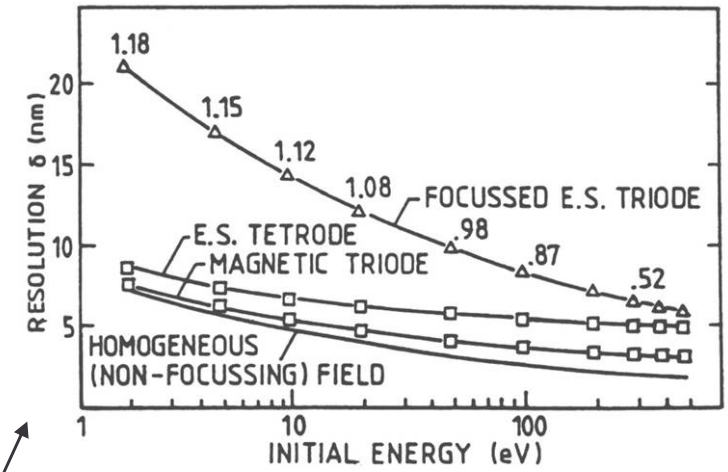


**ΔE-dependence at fixed E = 10 eV, $U_0$ = 18 kV magnetic triode**

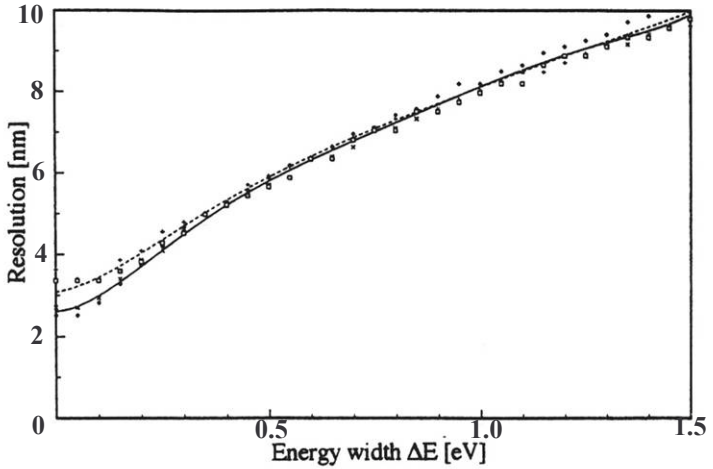

# Aberration correction in electron optics

Round **convex** lenses

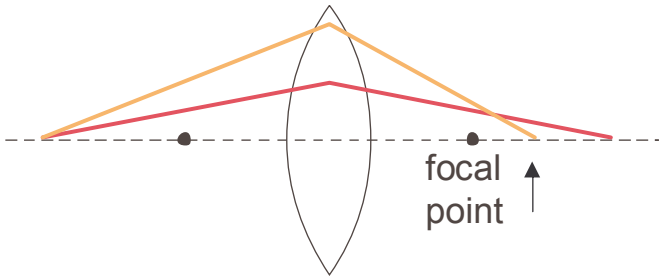


Spherical aberration

**electrostatic mirror**

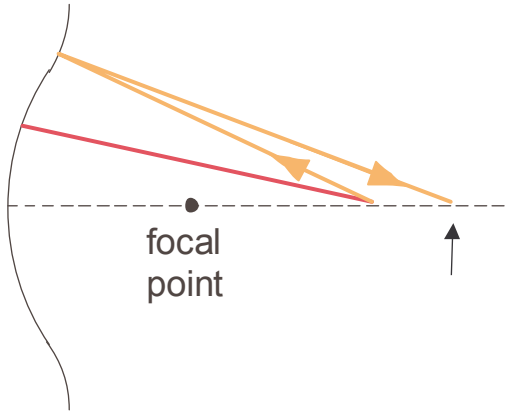


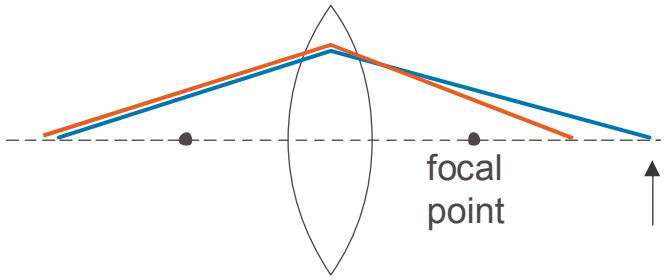


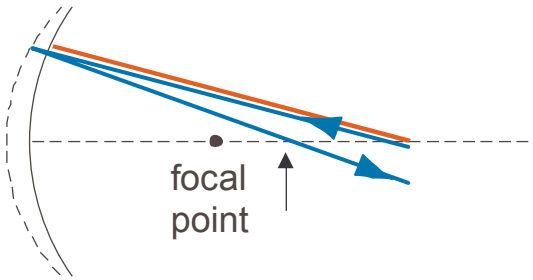


Chromatic aberration

Equipotential surfaces
in a diode mirror

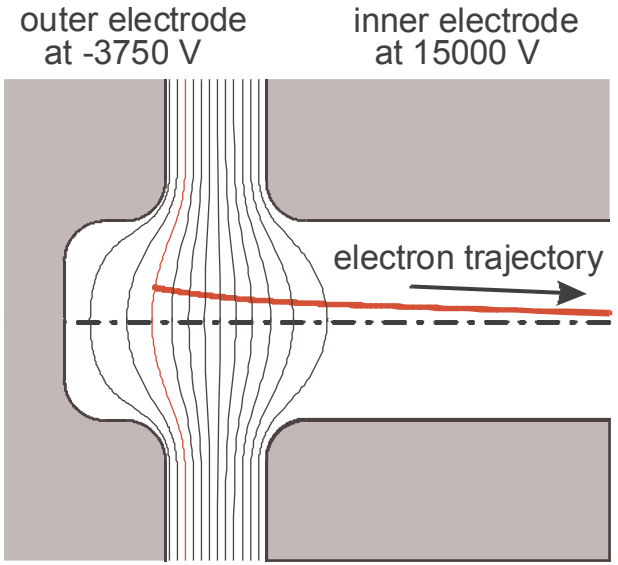

# Resolution improvement by aberration correction

## with electron mirror

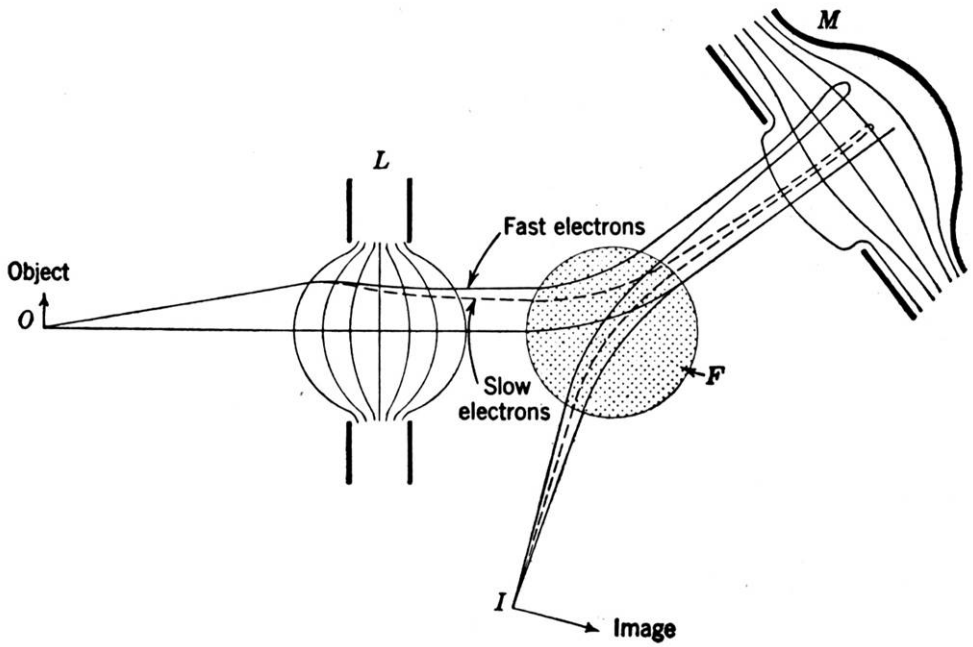


V.K. Zworykin et al, Electron Optics and the Electron Microscope, John Wiley, New York 1945

Recknagel 1935

# Resolution and transmission improvement with aberration correction

**Example: SMART**

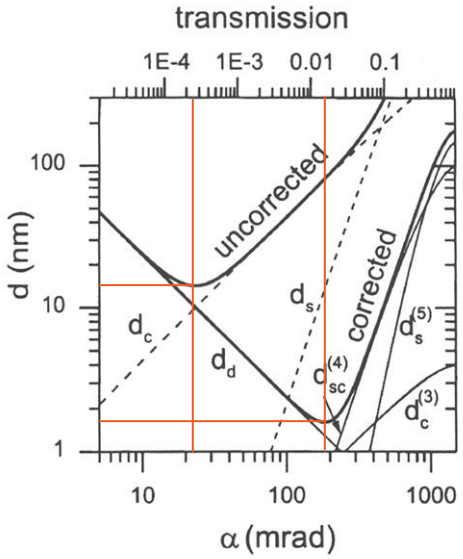


$E_0$ = 10 eV, ΔE = 2 eV, F = 5 kV/mm

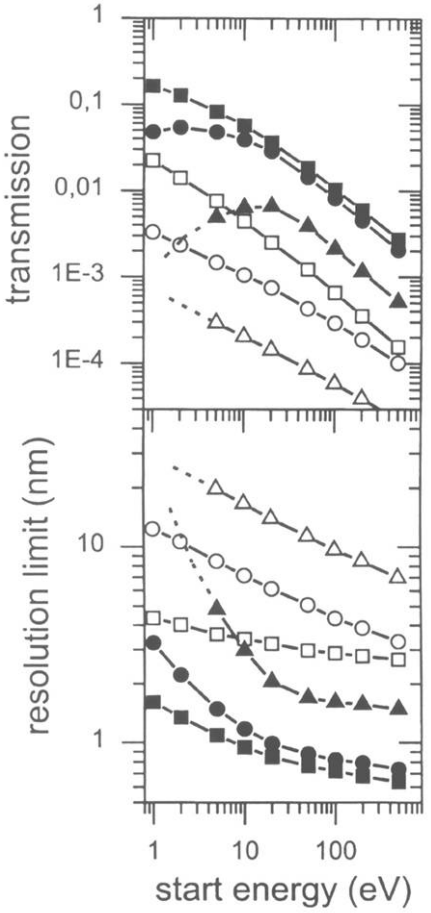


ΔE (eV)

0.1 □ ■

1.0 ○ ●

5.0 △ ▲

without correction | with correction

Calculations: D. Preikszas
From Th. Schmidt et al,
Surf. Rev. Lett. 9 (2002) 223

# Instruments

# Basic PEEM schematic

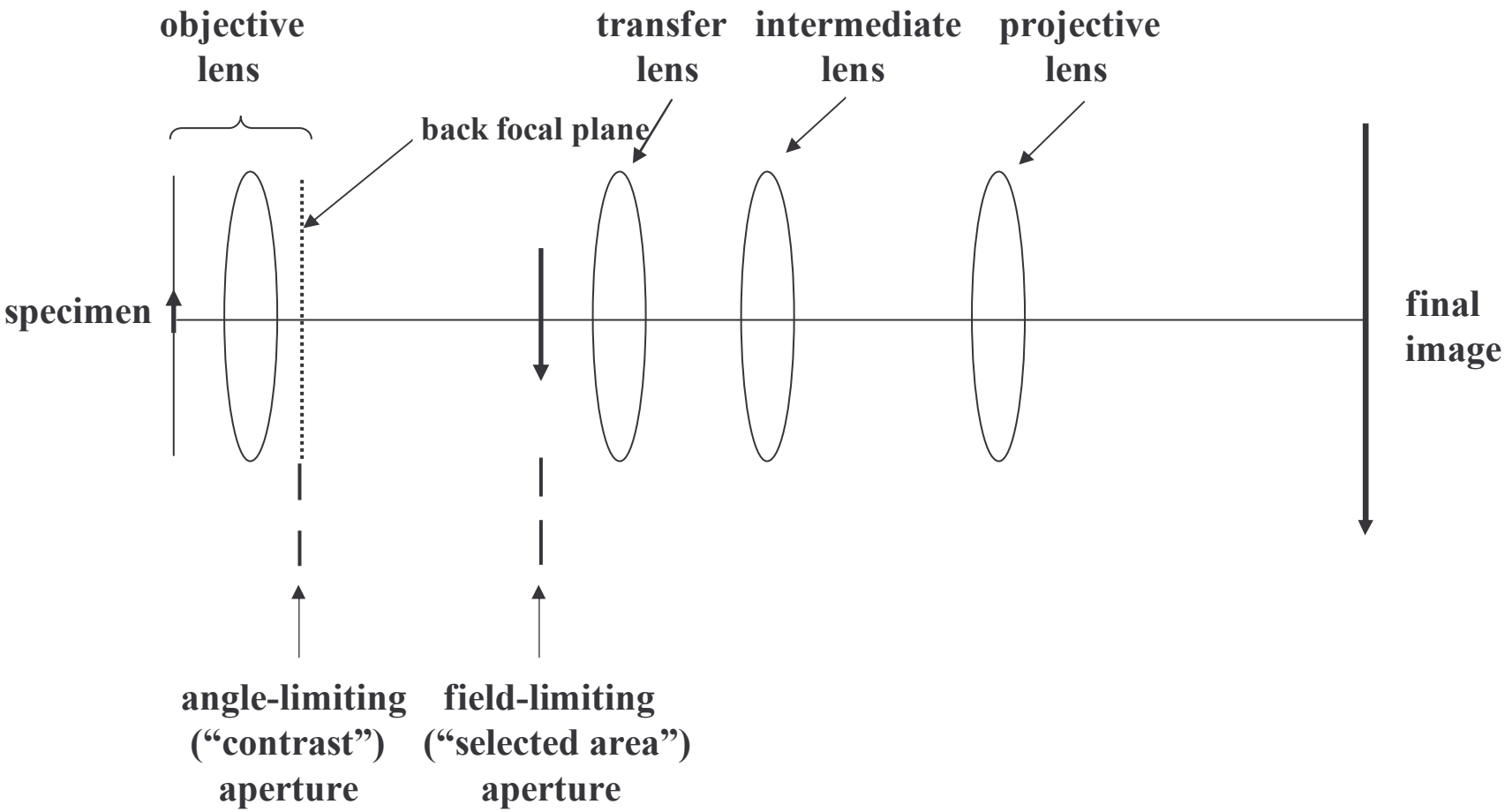

# Electrostatic PEEM examples

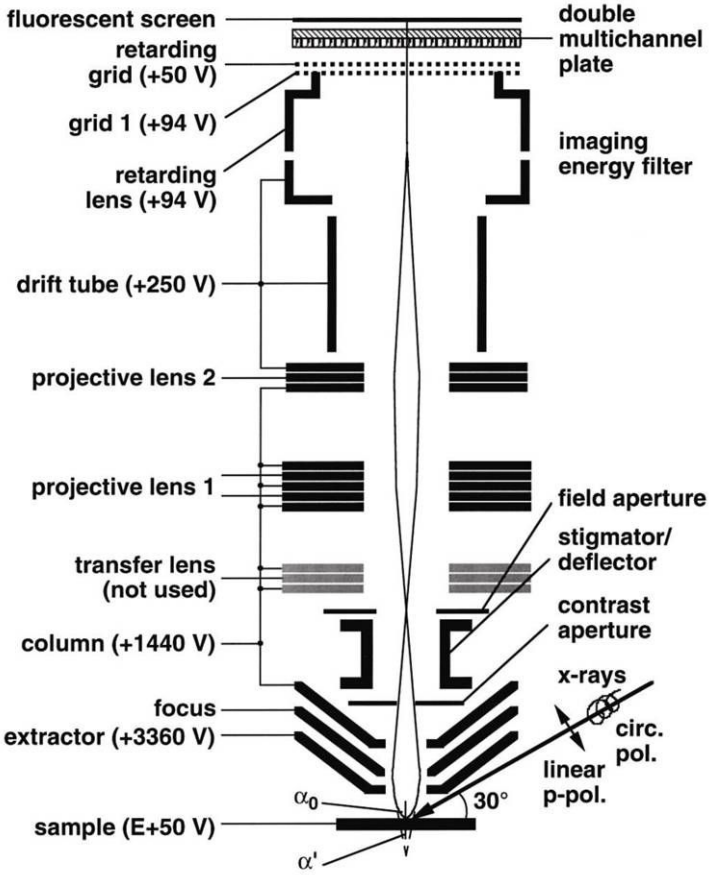


**Focus PEEM**
**with high pass filter**

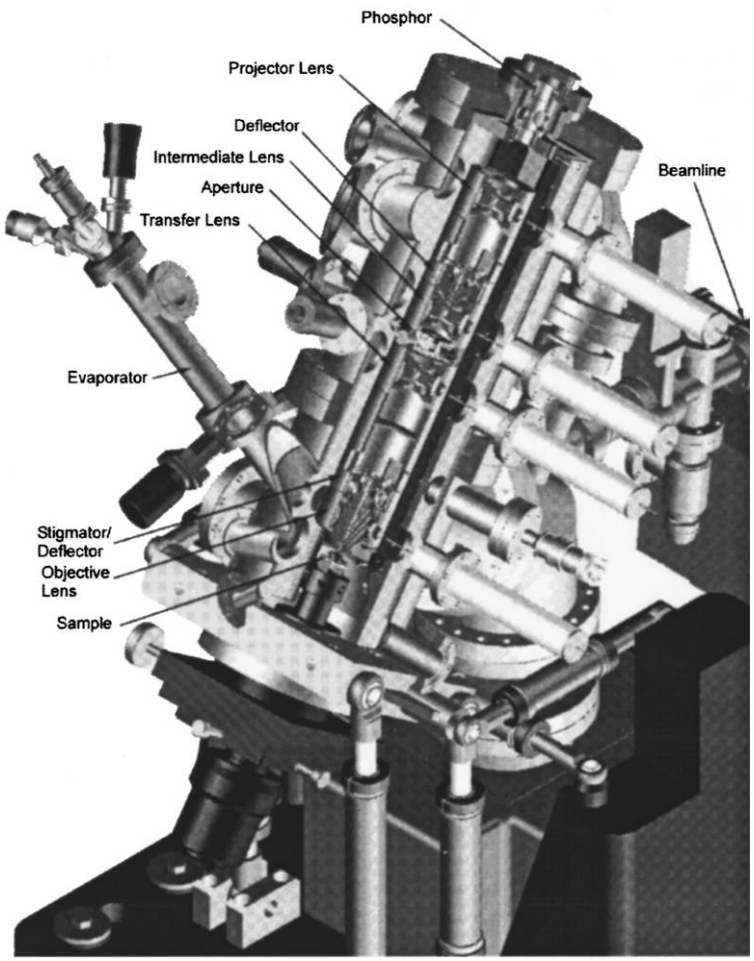


**ALS PEEM II**

# Magnetic PEEM (ELMITEC)

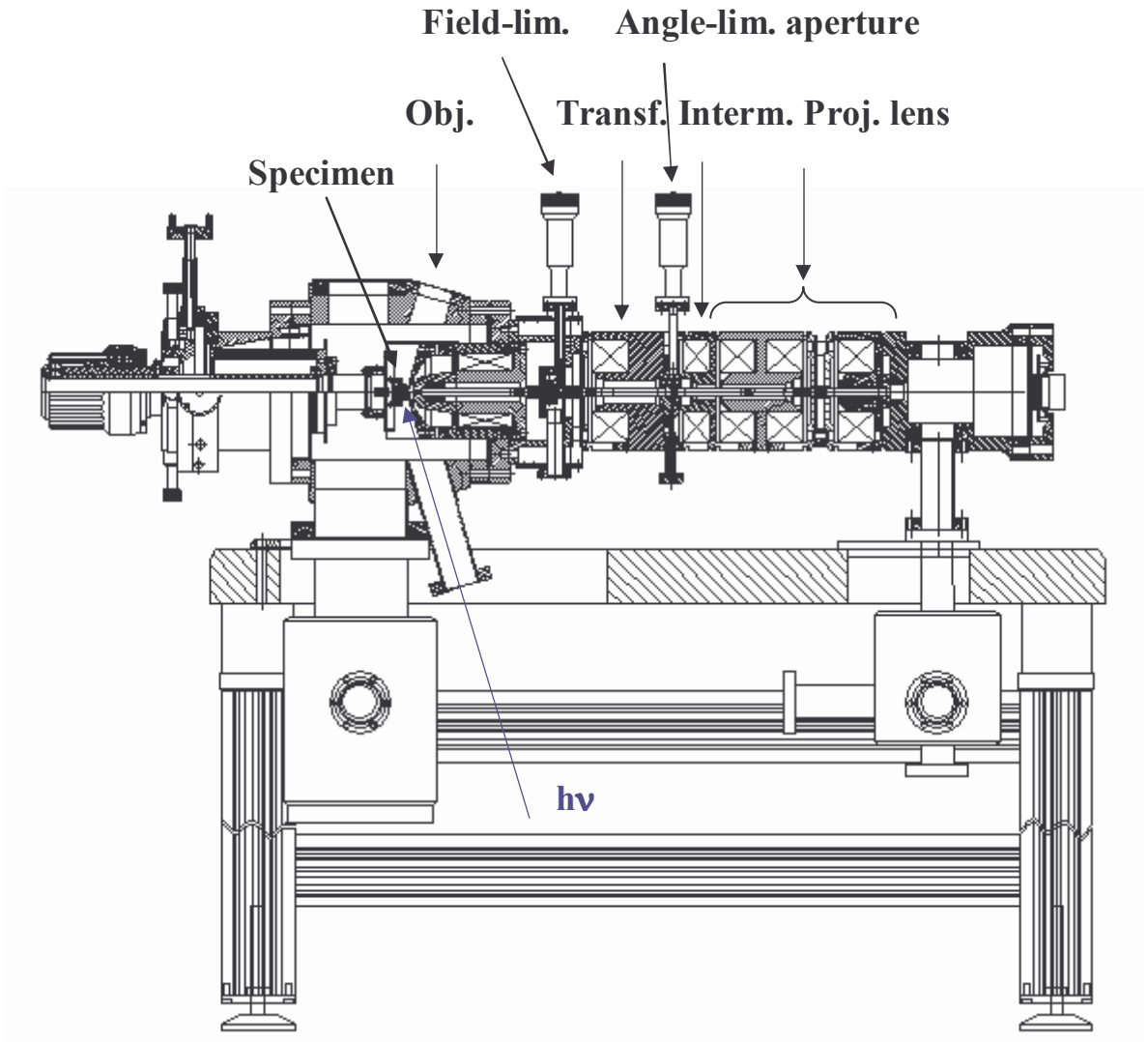

# Spectroscopic PEEM with band pass filter

**ELMITEC**

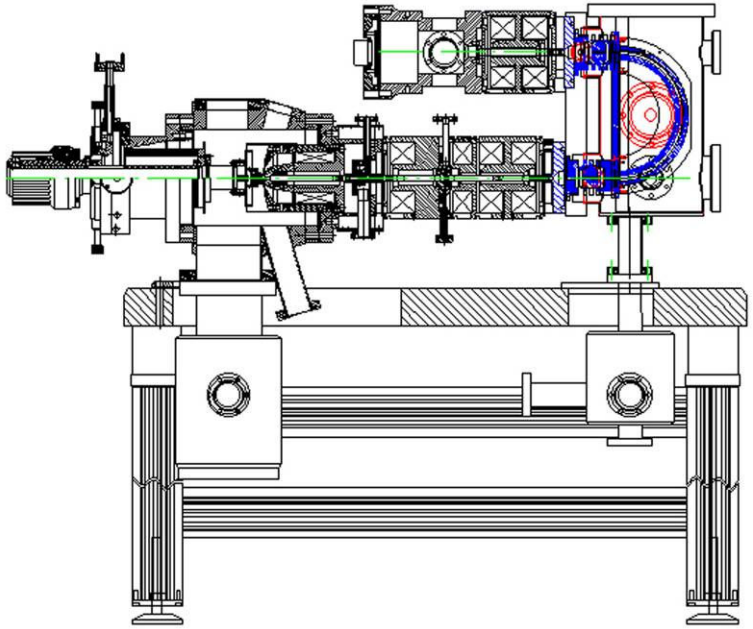

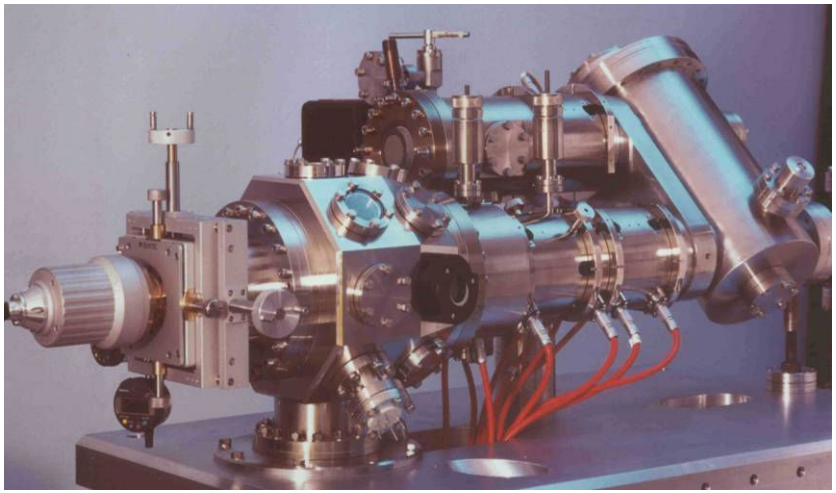

# Contrast mechanisms

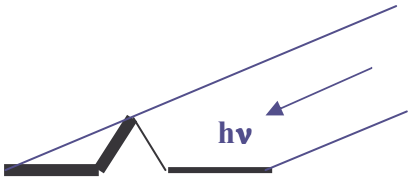


1 Topographic contrast due to oblique illumination and field distortion

2 Work function contrast at low $E_0$ (escape probability!)

3 Chemical contrast due to inner shell ionization

4 Magnetic contrast via XMCD and XMLD

No structural contrast, therefore combination with Low Energy Electron Microscopy (LEEM)

# Basic LEEM schematic

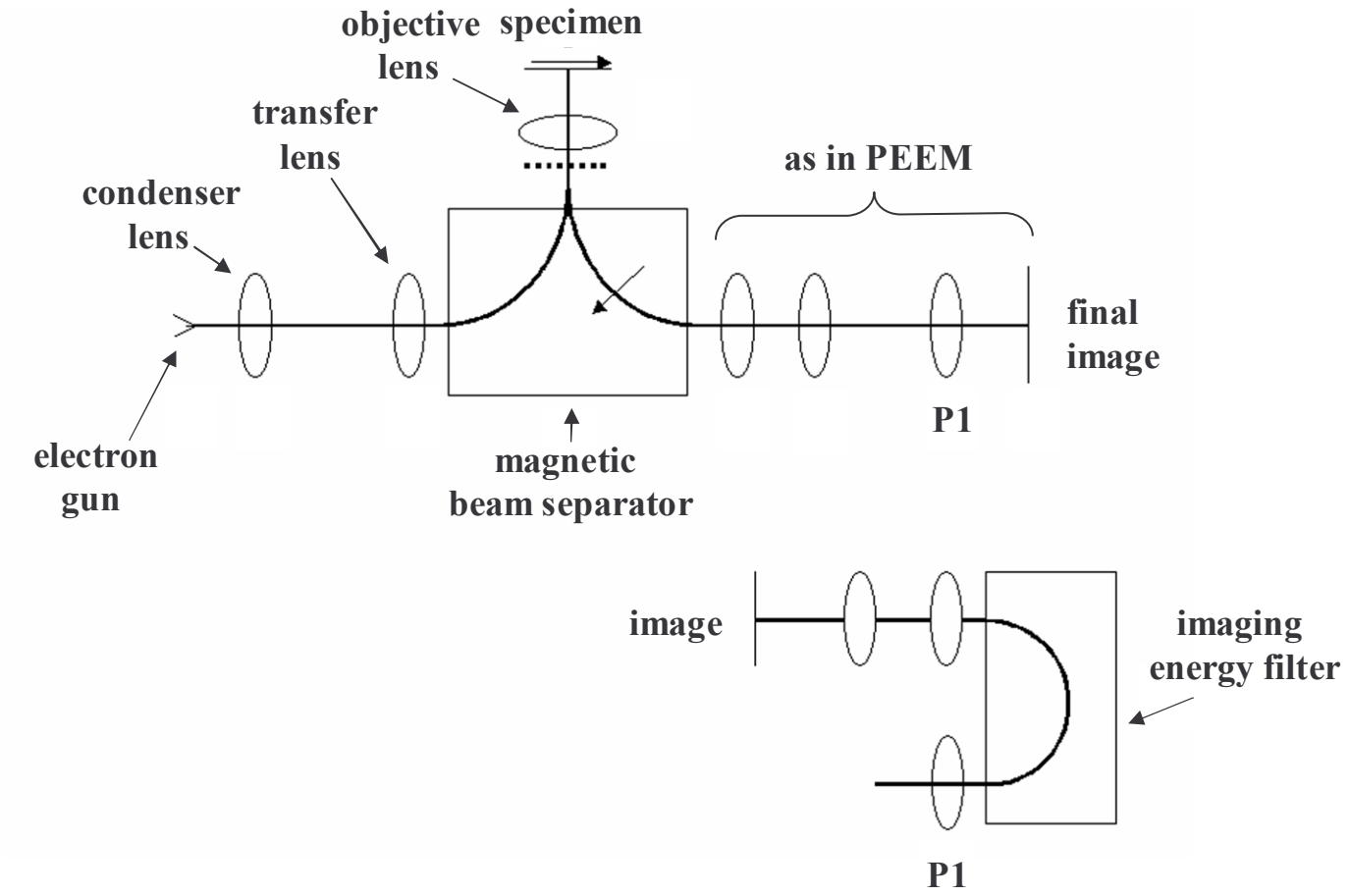

# Spectroscopic Photo Emission and Low Energy Electron Microscope

## SPELEEM

### ELMITEC

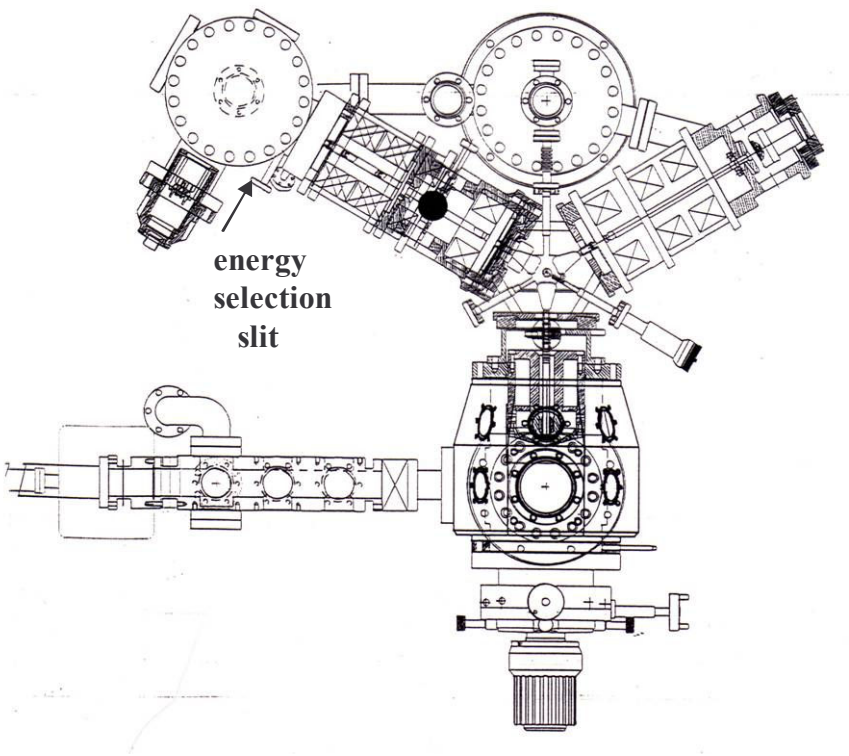


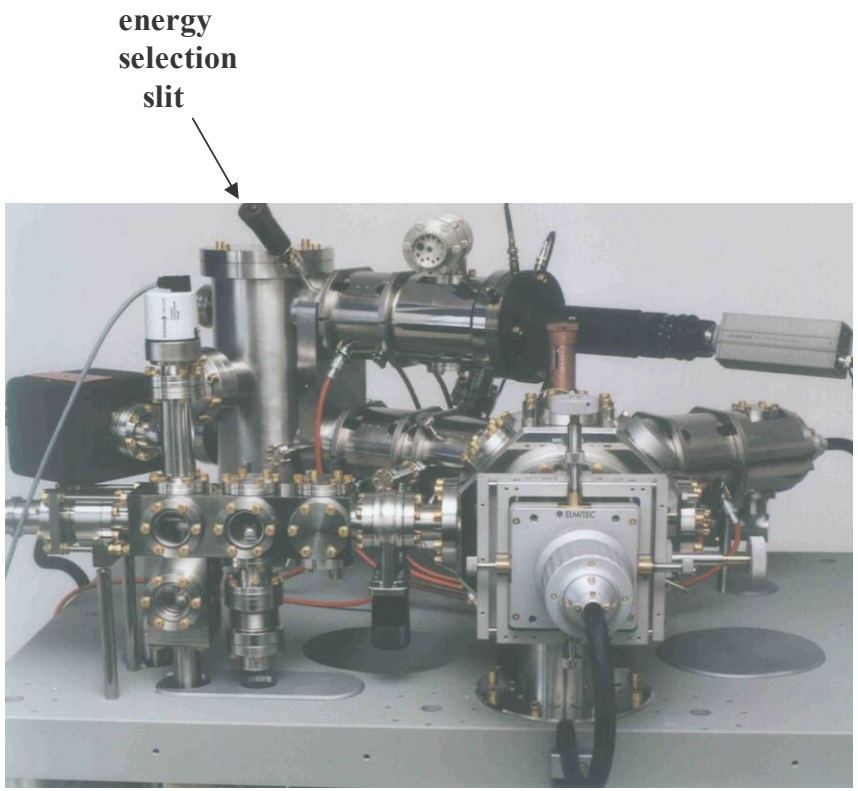

# LEEM with energy filter

## JEOL

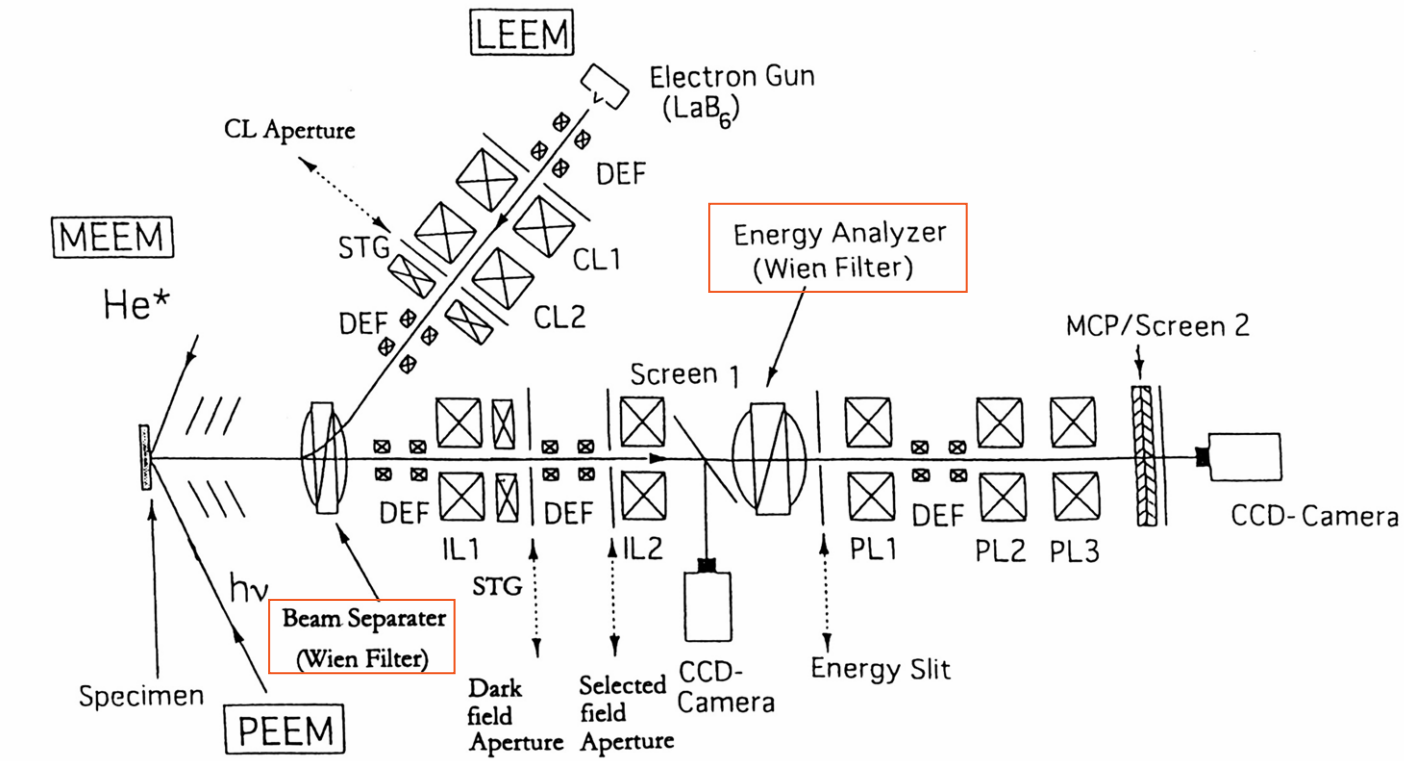


Y. Sakai et al, Surf. Rev. Lett. 5 (1998) 1199

# Aberration-corrected SPELEEM

## SMART (BESSY II)

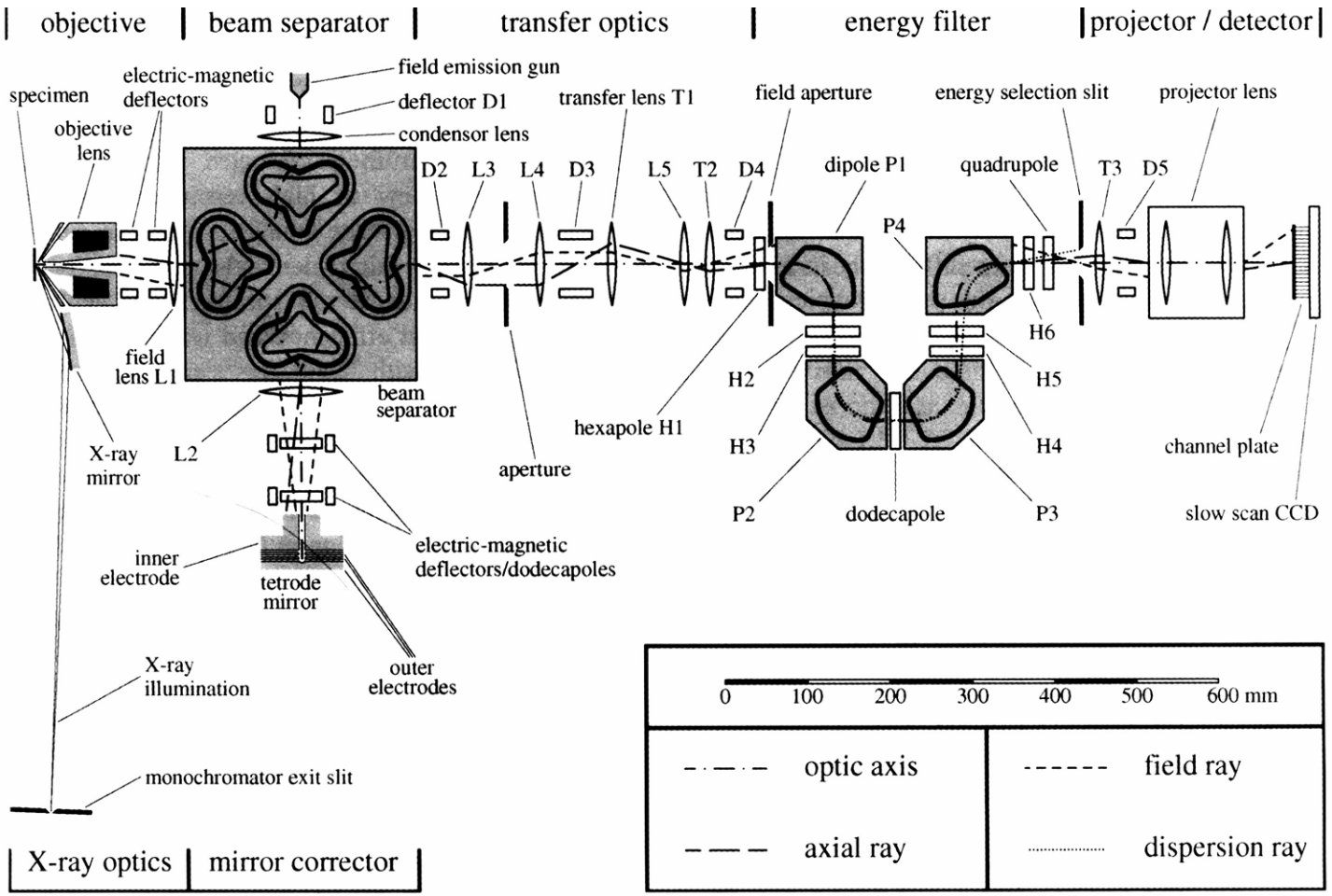


H. Rose, D. Preikszas, Nucl. Instr. & Meth. A363, 201 (1995)

# SMART side view

## Aberration corrected PEEM/LEEM with energy filtering

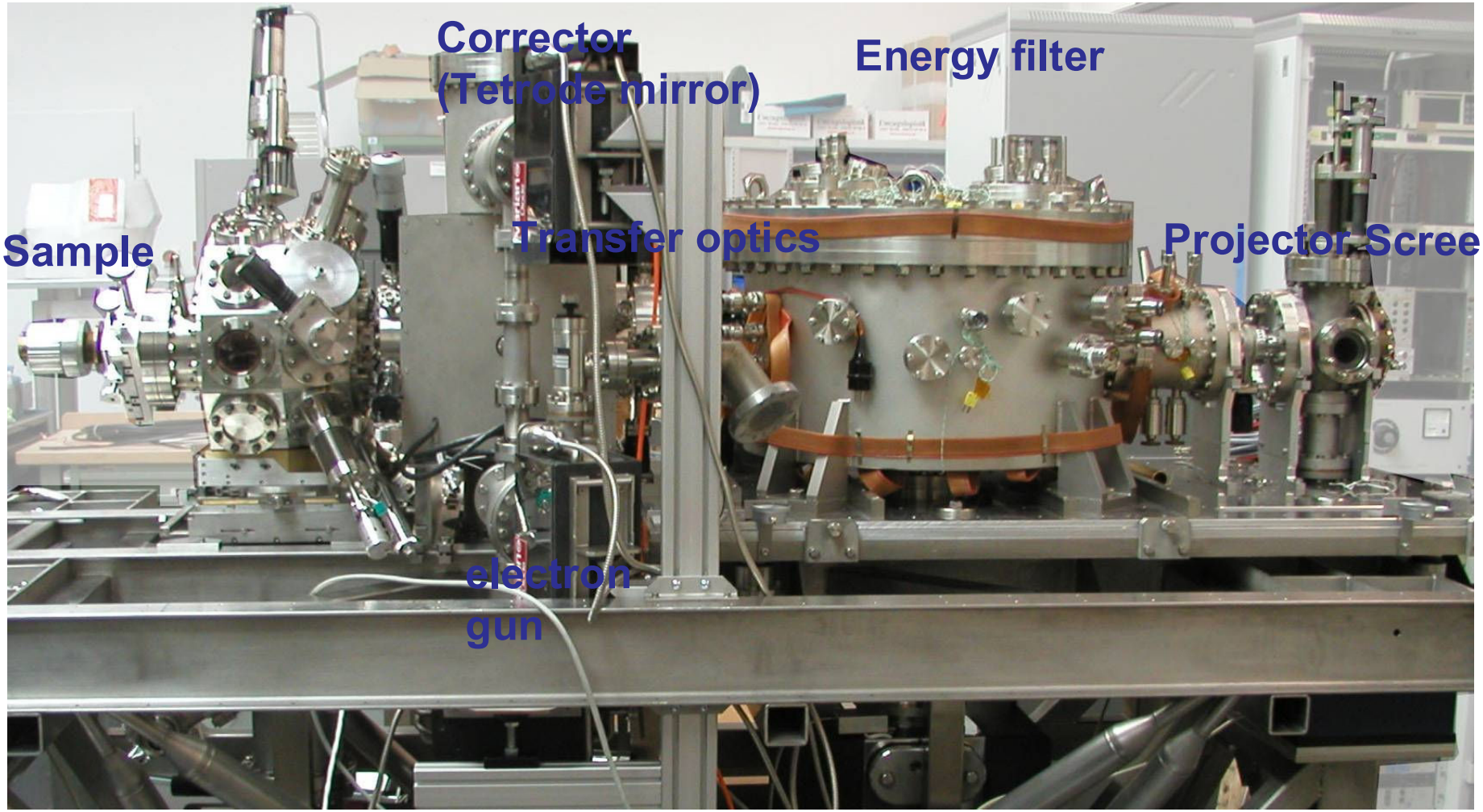


Th. Schmidt April 2004

# SMART top view

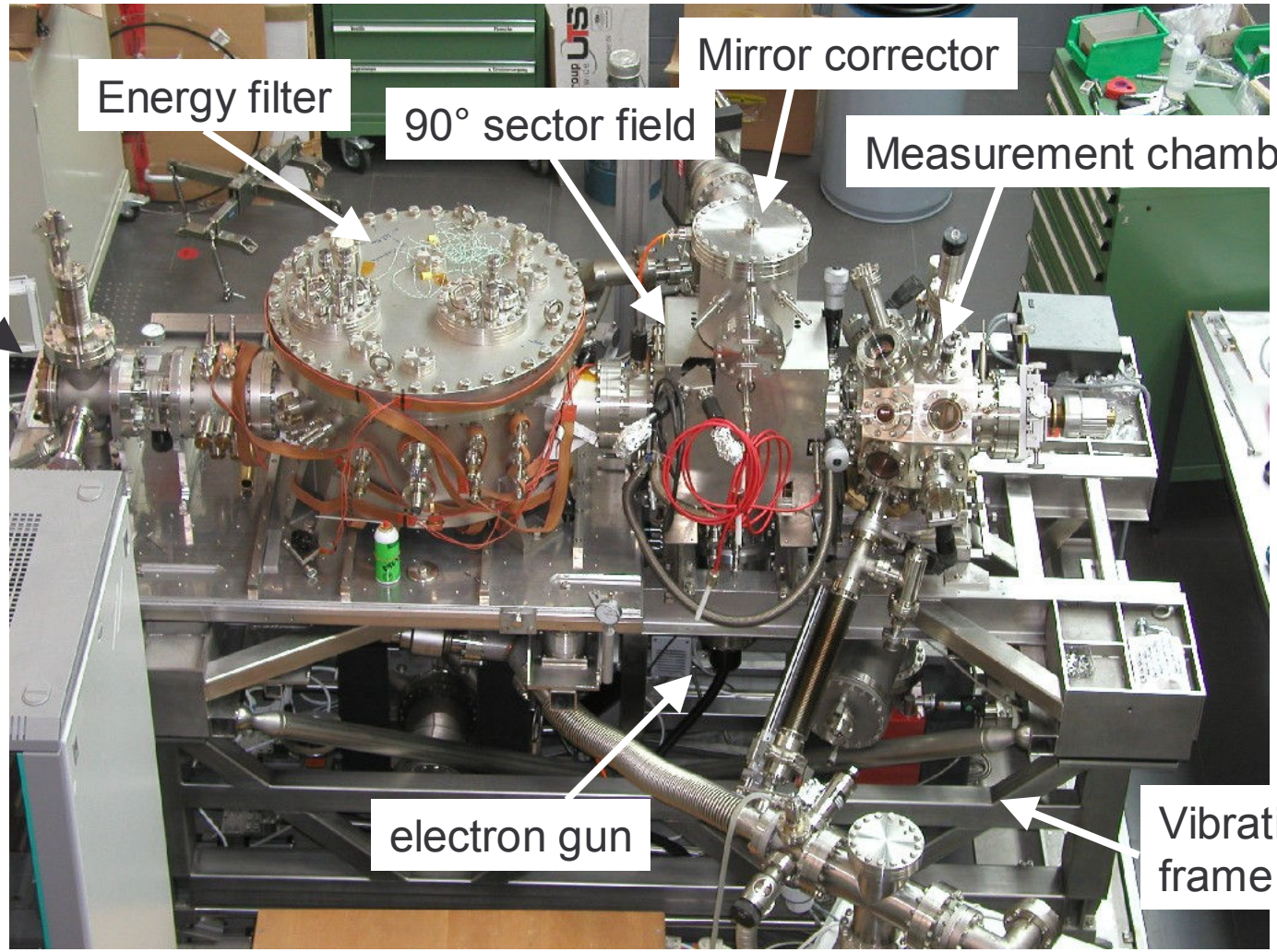


Th. Schmidt April 2004

# Methodic

# Operation modes of a SPELEEM

imaging

diffraction

spectroscopy

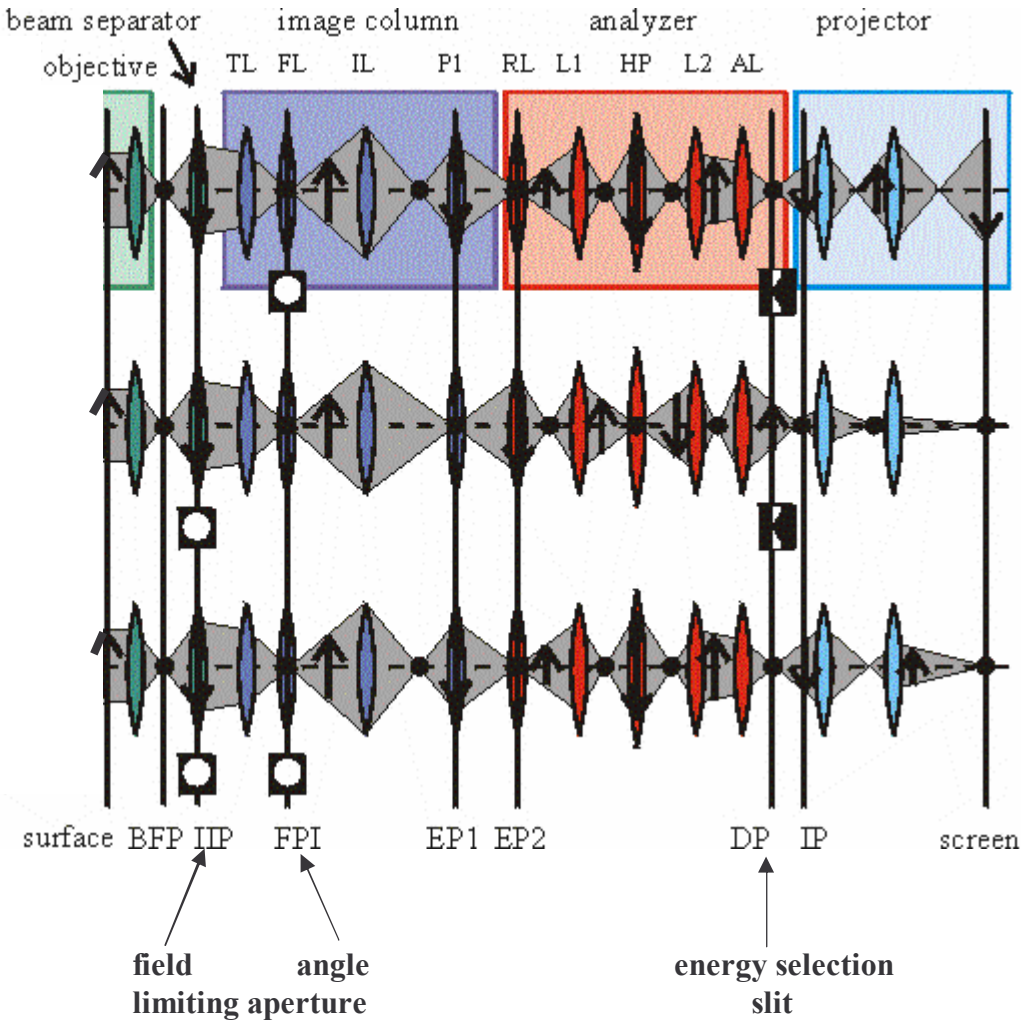


XPEEM

XPD (PED)

XPS (PES)
AES

Th. Schmidt et al, Surf. Rev. Lett. 5 (1998) 1287

# Operation modes of a SPELEEM

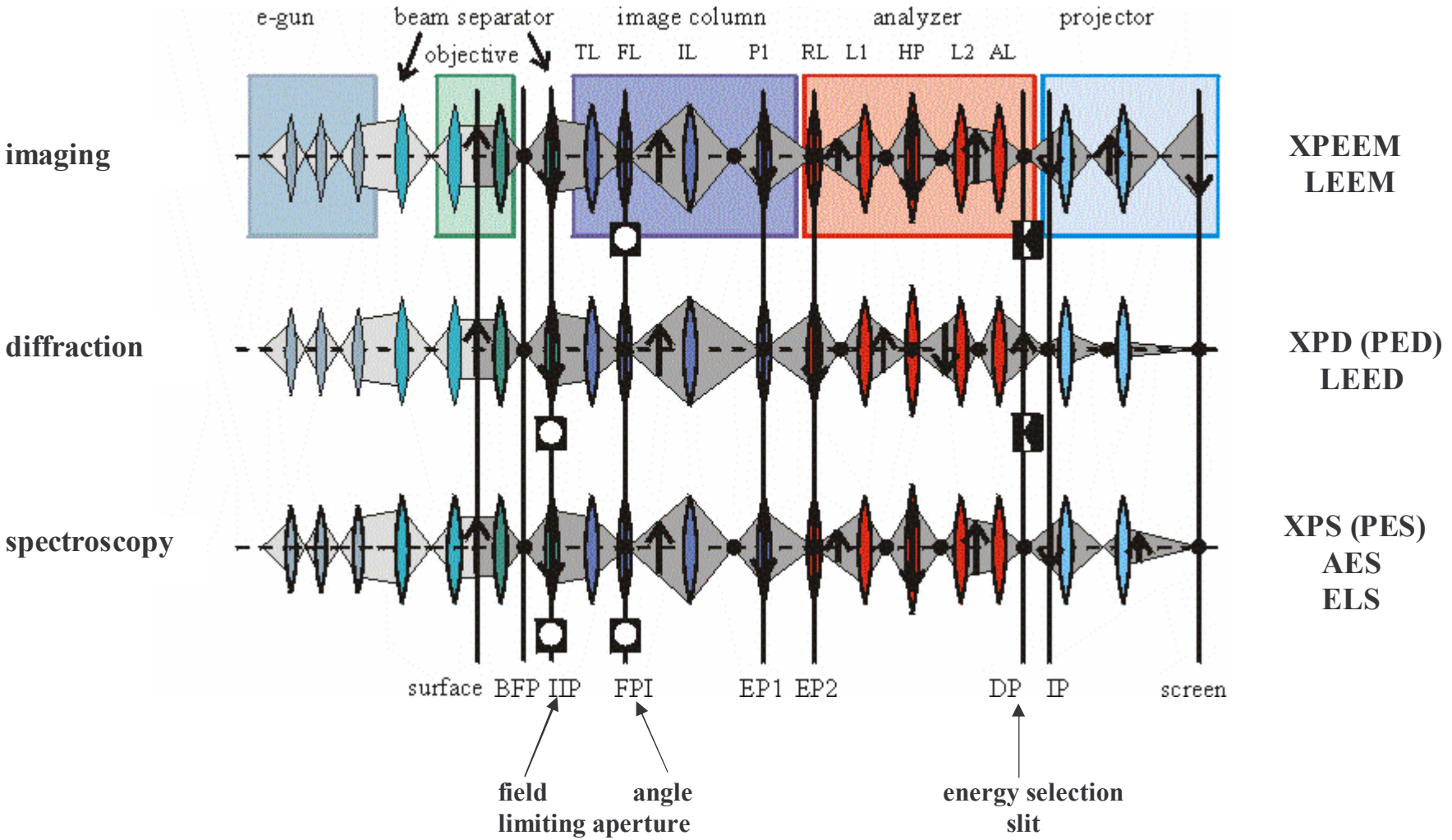


Th. Schmidt et al, Surf. Rev. Lett. 5 (1998) 1287

# PEEM practice

1 Ultrahigh vacuum (low $10^{-10}$ torr range)
but experiments up to $10^{-5}$ torr range possible

2 Surface cleaning: heating, sputtering or chemical
reactions, e.g with oxygen for carbon removal

3 Choice of optimum photon energy:

a. Secondary electron imaging: $h\nu \approx E_i$ (XANES, NEXAFS, XMCD, XMLD)

b. Photo electron imaging: $E_i + 30\ eV < h\nu < E_i + 100\ eV$

to minimize secondary electron background

to maximize transmission and photo electron yield

# Photo ionization cross sections

**Photon energy selection**

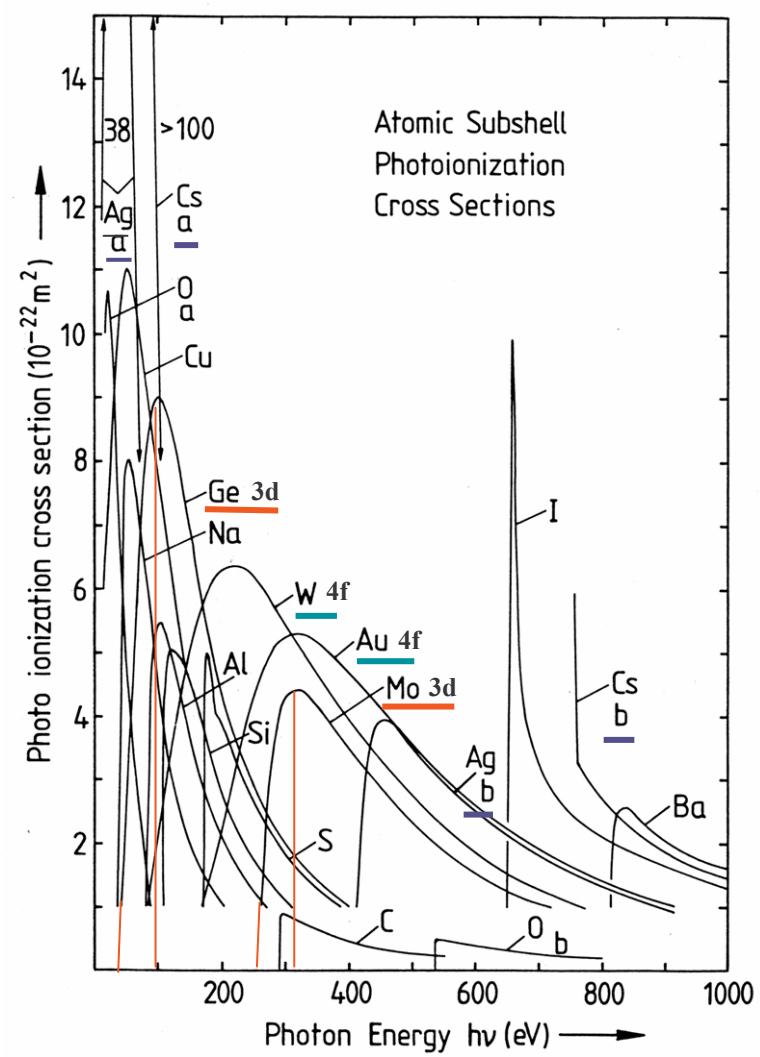


**Binding energies (eV)**

| | | |
|---|---|---|
| Ge 3d | | 29.8, 29.2 |
| Mo 3d | | 231.1, 227.9 |
| W 4f | | 33.6, 31.4 |
| Au 4f | | 87.6, 84.0 |
| Ag | | |
| a | 4d | ≈ 5 |
| b | 3d | 374.0, 368.3 |
| Cs | | |
| a | 4d | 79.8, 77.5 |
| b | 3d | 740.5, 726.6 |

J.J. Yeh and I. Lindau,
Atomic Data 1985

# The usefulness of LEEM

## Properties not visible with PEEM, but with LEEM

**atomic steps**

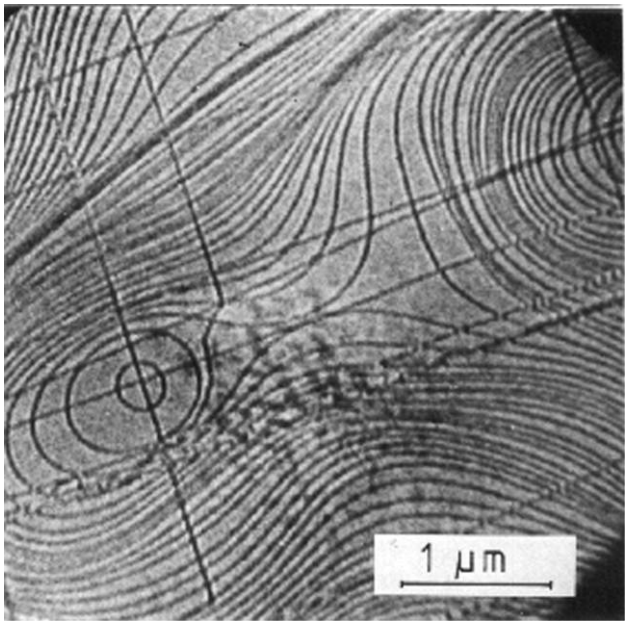


Mo(110)

**interference contrast**

**domain orientations**

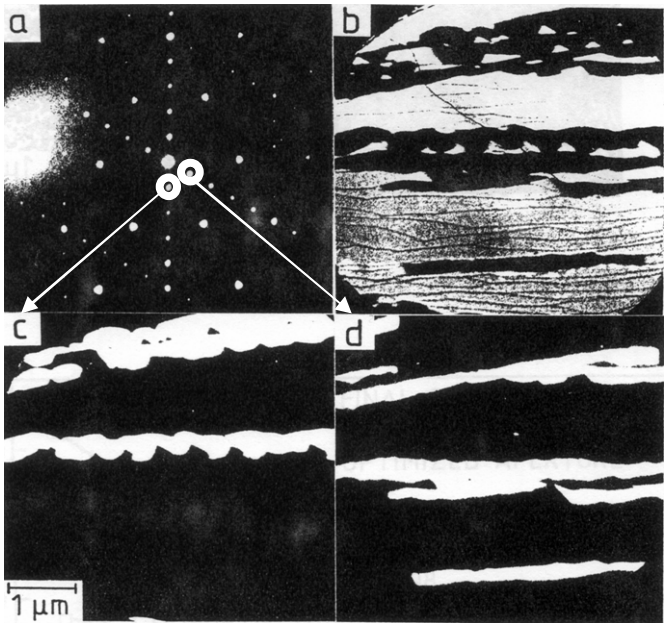


Au($\sqrt{3}\times\sqrt{3}$)-R30° + Au(5 ×2) on Si(111)

b c,d

**diffraction contrast**

**LEEM also much brighter and better resolution ⇒ use for focusing in XPEEM**
**LEED much easier to interpret than PED ⇒ use for structure analysis**

# Classical emission microscopy

**Polycrystalline tantalum**

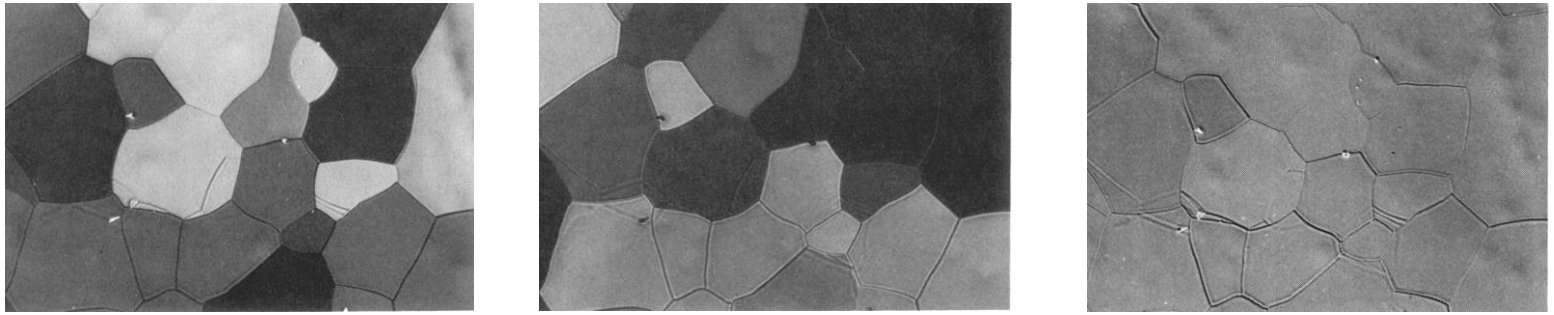

20 µm

thermionic emission | threshold photo emission | secondary emission

**Photo emission from polycrystalline beryllium bronce**

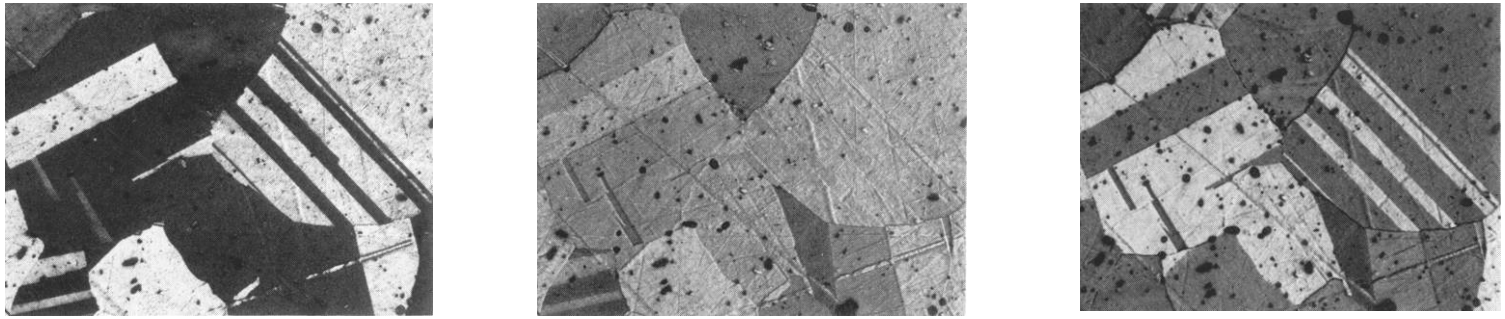

10 µm

low | medium | high

energy region of the UV spectrum of a Hg high pressure lamp

W. Engel, Ph.D. thesis, TU Berlin 1968

# Operation modes of a SPELEEM

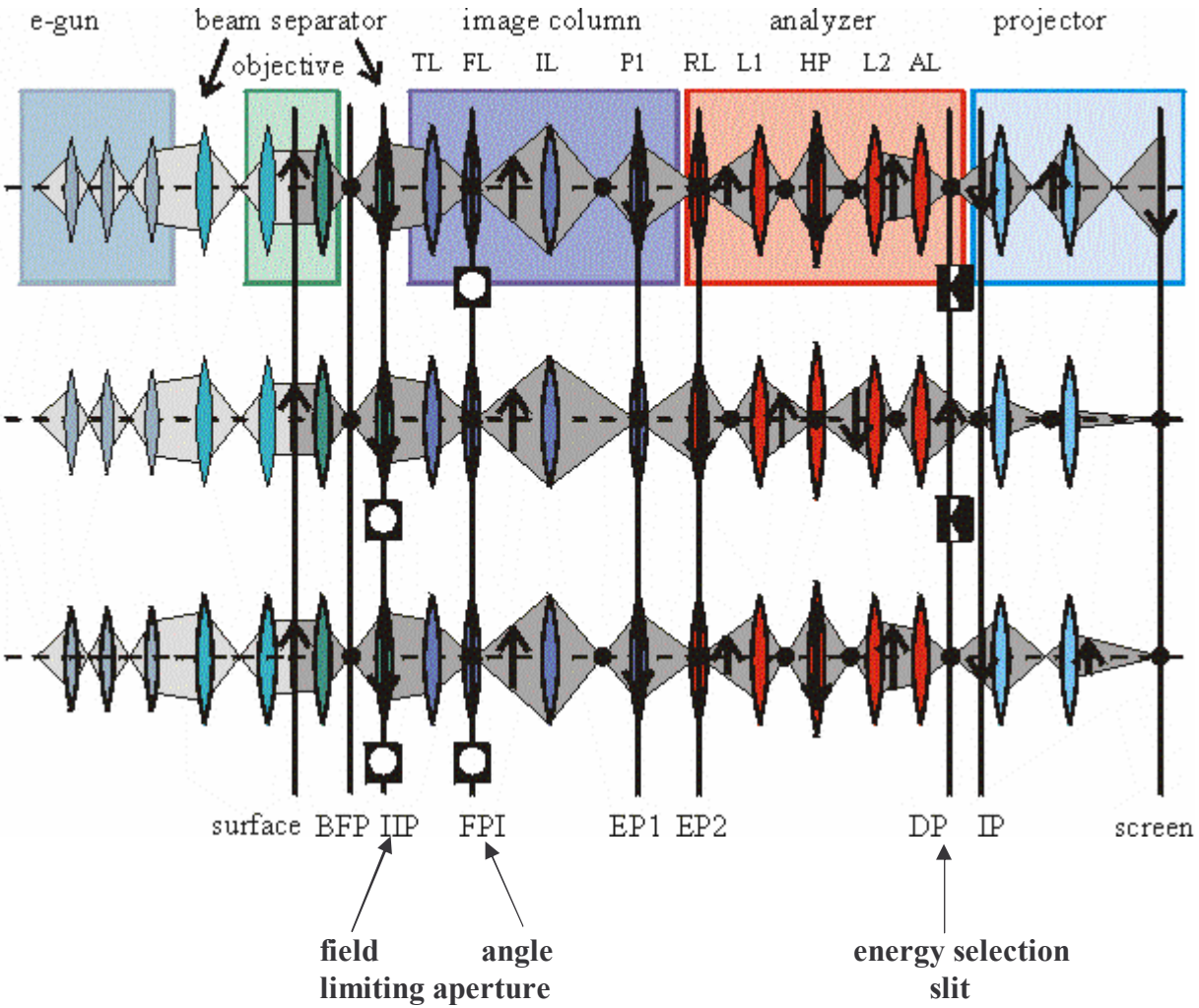


**imaging**

**mode 1**

**diffraction**

**spectroscopy**

**XPEEM**
**LEEM**

**XPD (PED)**
**LEED**

**XPS (PES)**
**AES**
**ELS**

Th. Schmidt et al, Surf. Rev. Lett. 5 (1998) 1287

# Chemical imaging (mode 1)

**secondary electrons**
**spatial resolution**
$\sigma_{Ag4d} \approx 5\,\sigma_{W5d}$
$h\nu = 65$ eV $>> E_i < 10$ eV
$\Delta E_F \leq 1$ eV

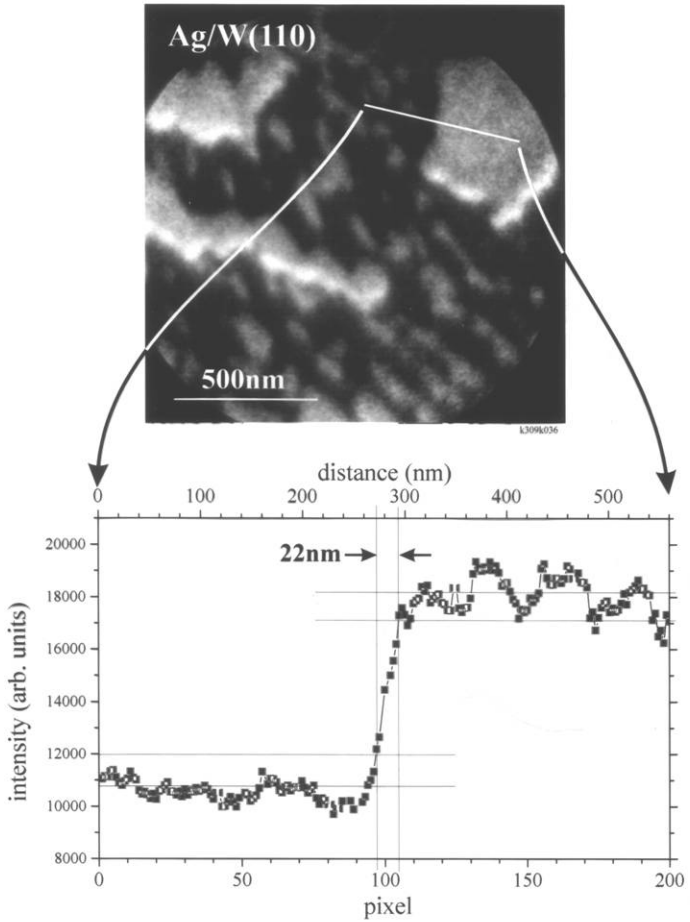


**photo electrons**
**energy resolution**
$h\nu = 65$ eV, images in 0.2 eV steps
10-60 sec/image 0.25 $\mu m^2$ areas
$\Delta E_F \leq 0.5$ eV, $\Delta E_{chem} \approx 0.15$ eV

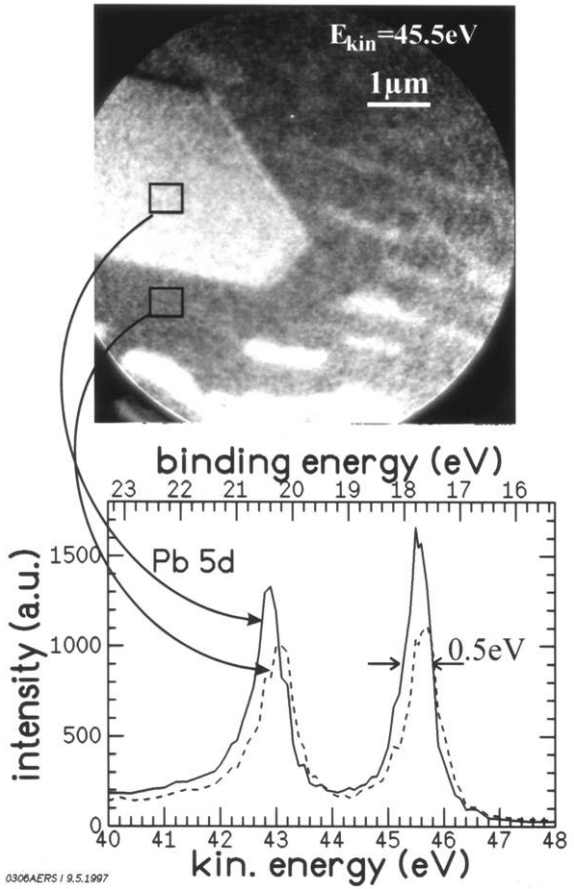


Pb/W(110)

Th. Schmidt et al, Surf. Rev. Lett. 5 (1998) 1287

# Operation modes of a SPELEEM

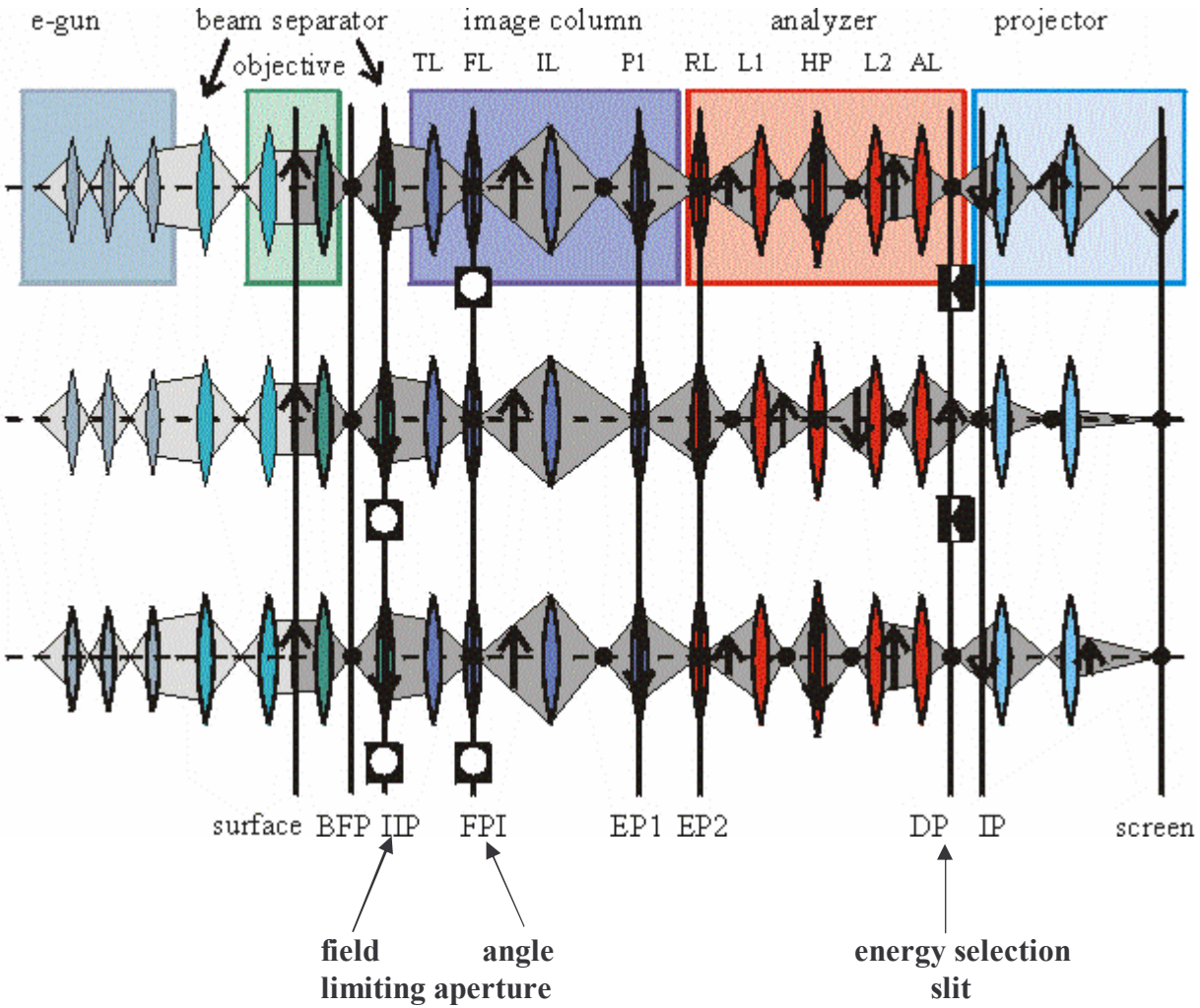


**imaging**

**diffraction**

**spectroscopy**

**mode 3**

**XPEEM**
**LEEM**

**XPD (PED)**
**LEED**

**XPS (PES)**
**AES**
**ELS**

Th. Schmidt et al, Surf. Rev. Lett. 5 (1998) 1287

# Fast local spectroscopy
## by imaging the dispersive plane (mode 3)

**$\alpha$= 8$^o$ (contrast aperture), 0.8 $\mu$m$^2$ area (selected field aperture)**
**20 eV full dispersion, 60 sec**
**h$\nu$ = 48 eV**

**8 monolayers Pb on Si(111)-$\sqrt{3}\times\sqrt{3}$-Ag**

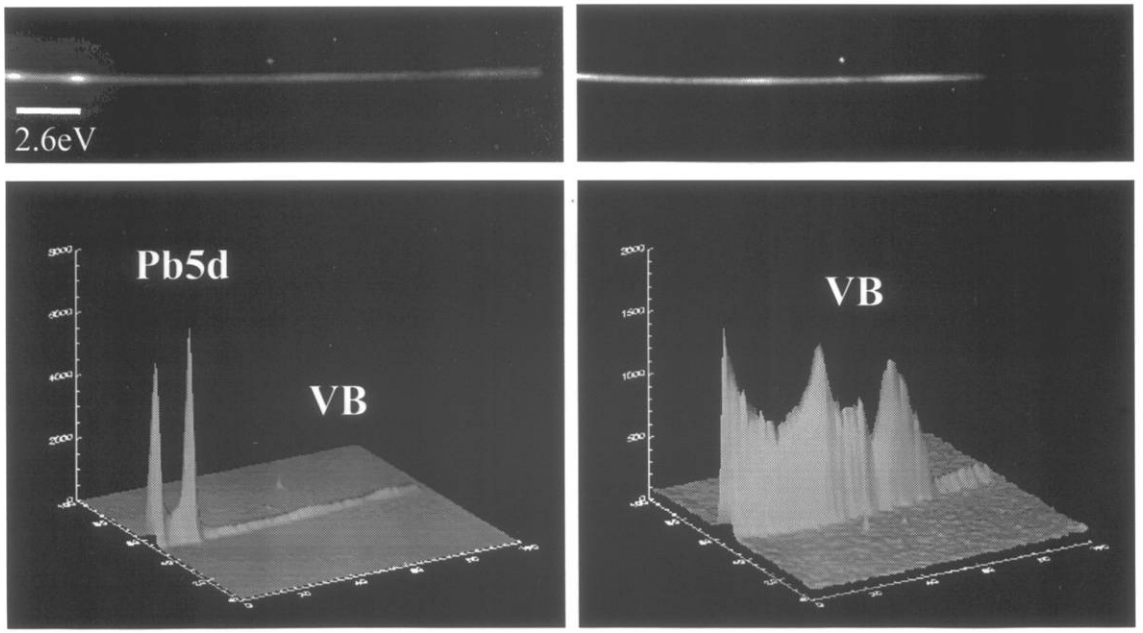


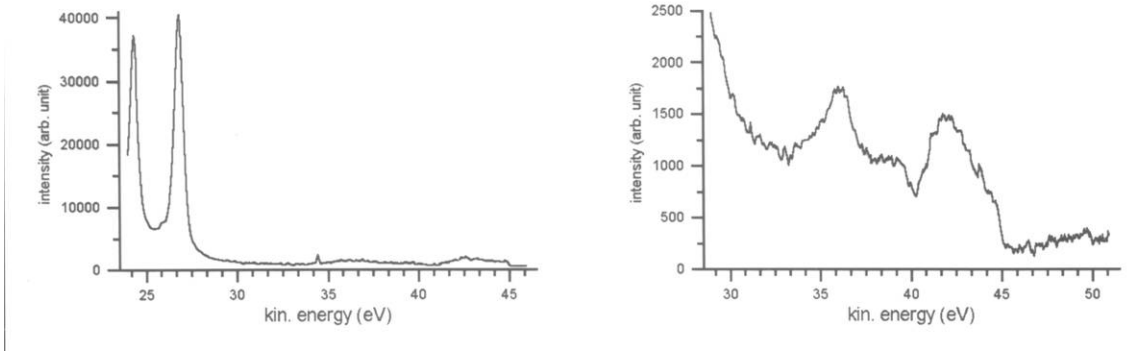


Th. Schmidt et al, Surf. Rev. Lett. 5 (1998) 1287

# Surface sensitivity of photo electrons

**versus secondary electrons**

**valence band region**

**hν = 48 eV**

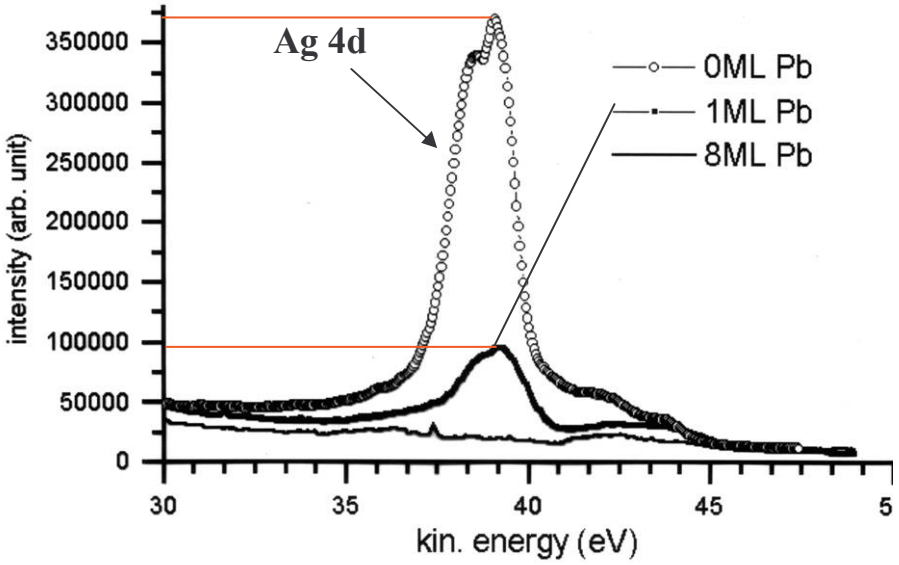


**Pb on Si(111) – Ag (√3×√3) – R30°**
**(1 monolayer Ag)**

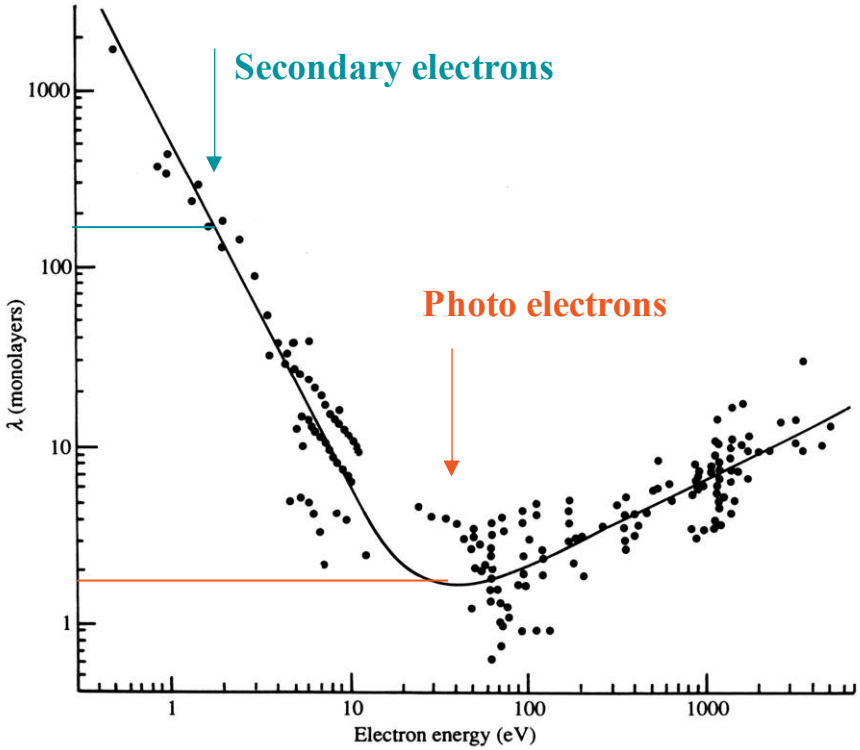


**Inelastic mean free path**
**("universal curve")**
**determines sampling depth**

**Th. Schmidt et al, 1998**

# Operation modes of a SPELEEM

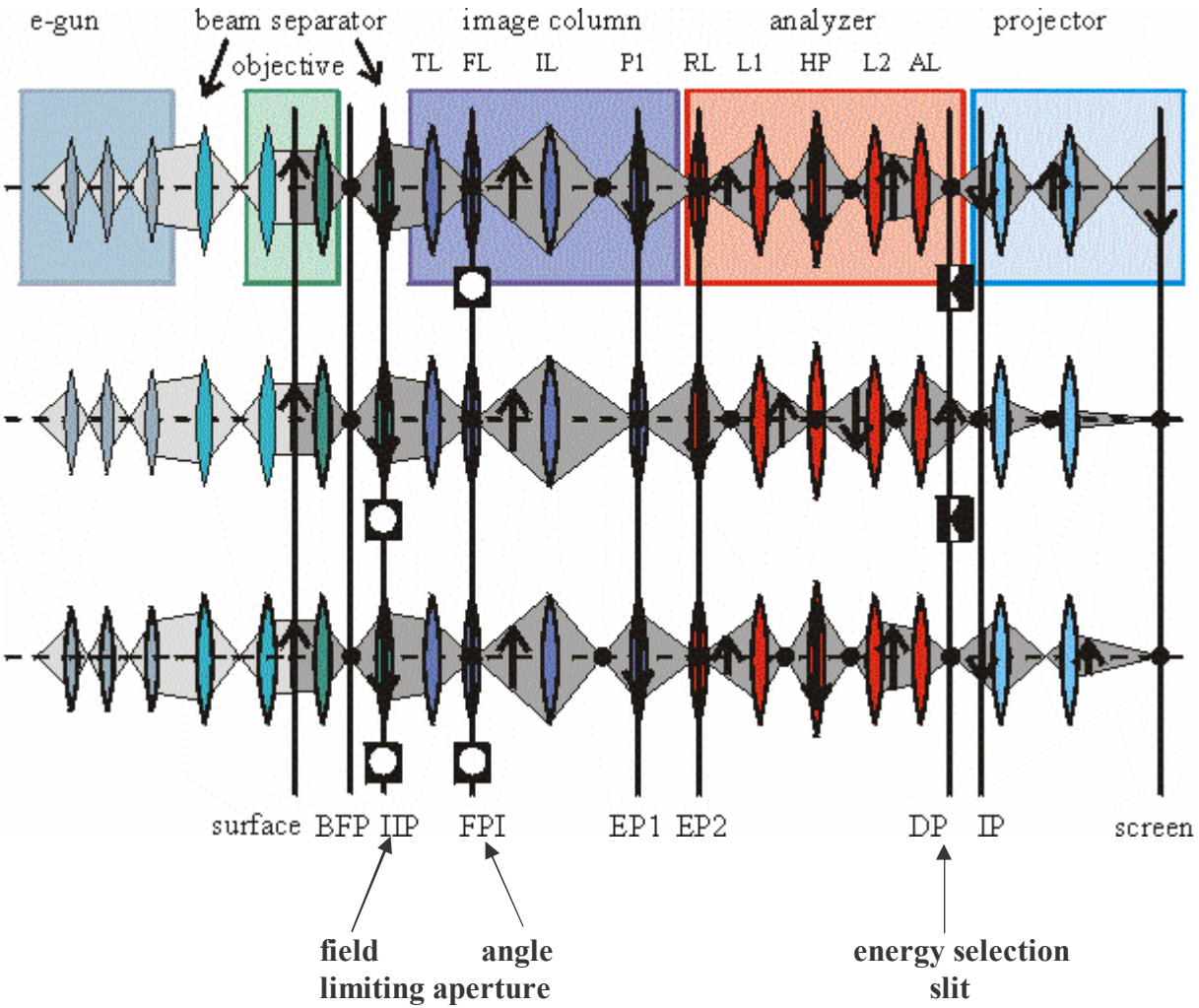


**imaging**

**diffraction**

**mode 2**

**spectroscopy**

**XPEEM**
**LEEM**

**XPD (PED)**
**LEED**

**XPS (PES)**
**AES**
**ELS**

Th. Schmidt et al, Surf. Rev. Lett. 5 (1998) 1287

# Local photo electron diffraction (mode 2)

**Pb 5d photo electrons**

**from 0.8 μm² area (selected field aperture)**

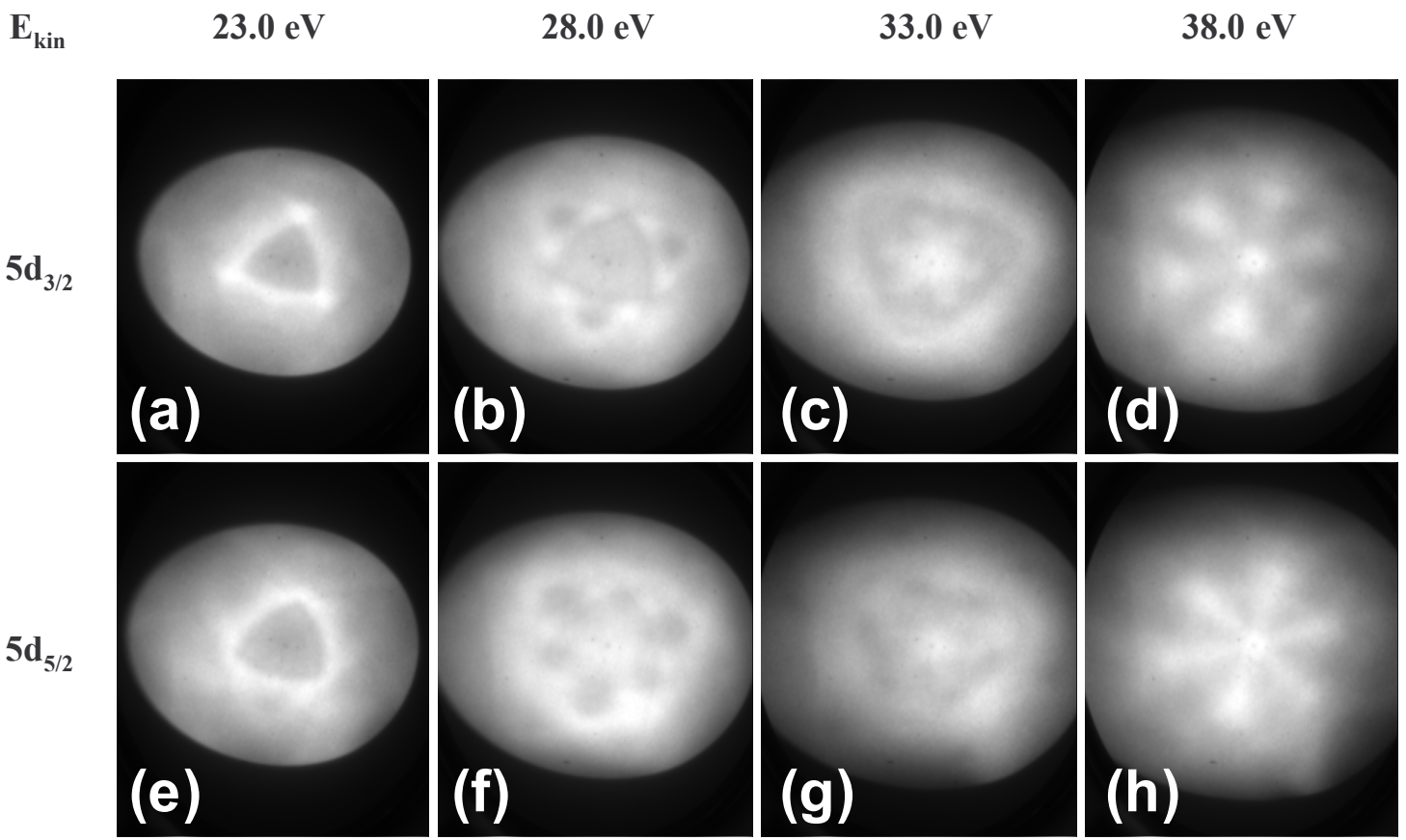


Th. Schmidt et al, Surf. Rev. Lett. 5 (1998) 1287

# Local band structure analysis (mode 2)

**Conduction band of Pb(111)**

**5 Pb monolayers on Si(111) – Au $\sqrt{3}\times\sqrt{3}$ – R30°**

**$h\nu$ = 73 eV, 0.8 $\mu m^2$ area (selected field aperture)**

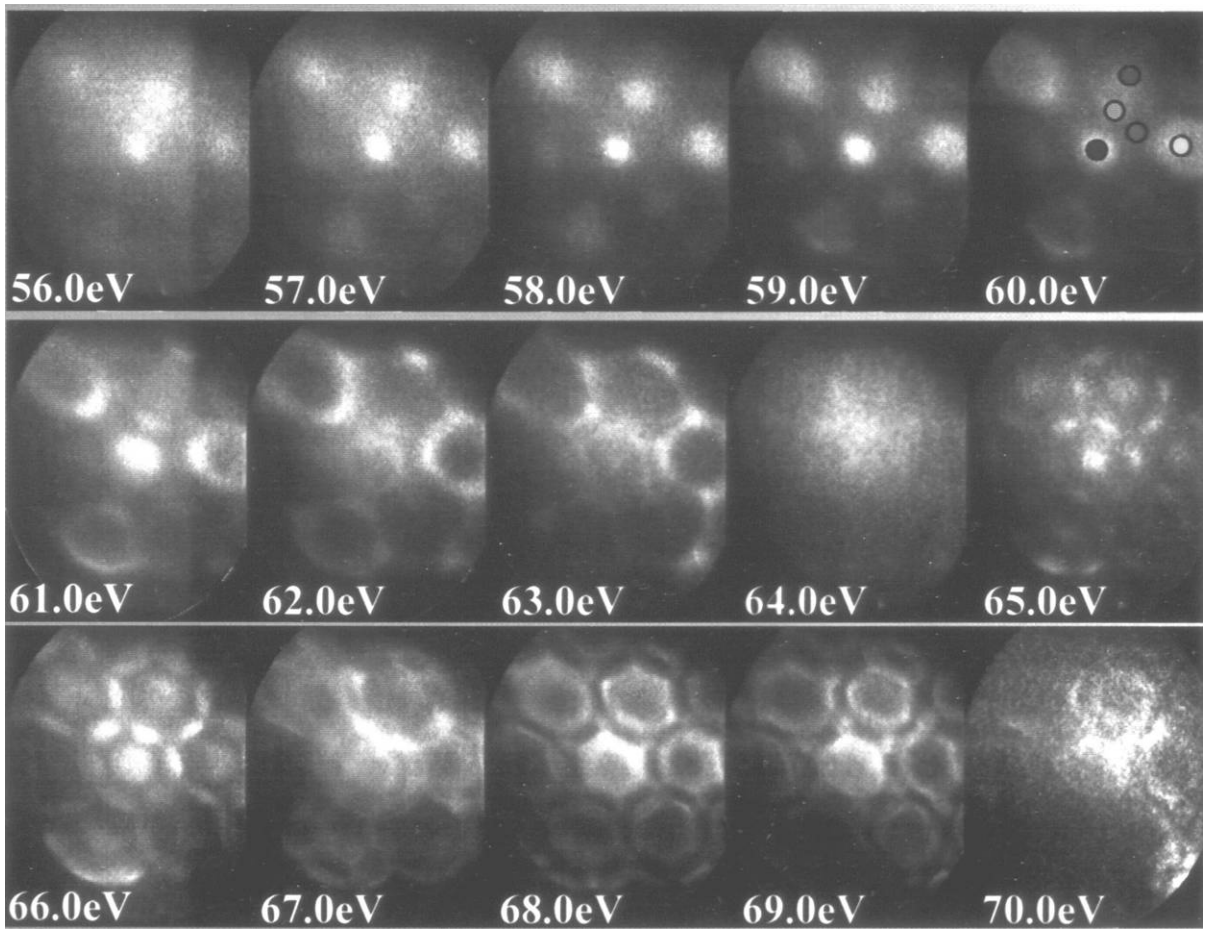


**Parameter: $E_{kin}$**

**Th. Schmidt, 1997**

# Application examples

# Fe on Pb on W(100)

## Surfactant action

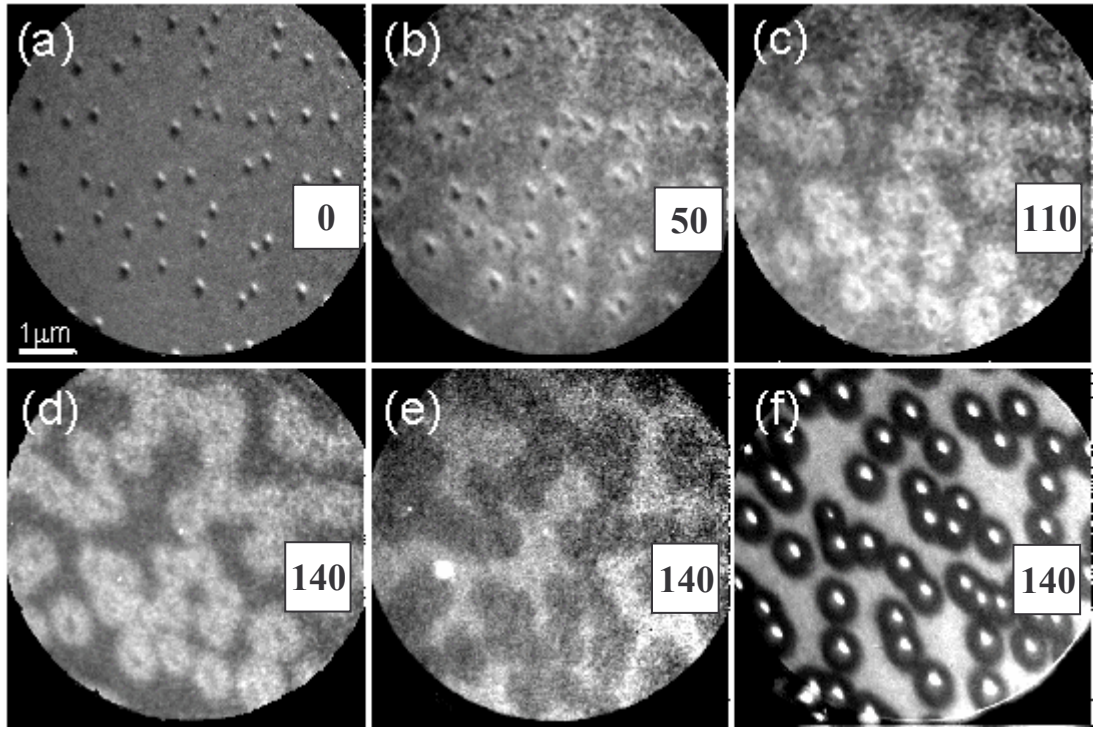


**(a) – (d) Pb 5d images ($h\nu$ = 70.5 eV, $E_{kin}$ = 49 eV, (e) Fe 3d image, (f) LEEM image 270 K**

**Th. Schmidt et al, 1999**

# InAs nanocrystals on Se-passivated GaAs(100)

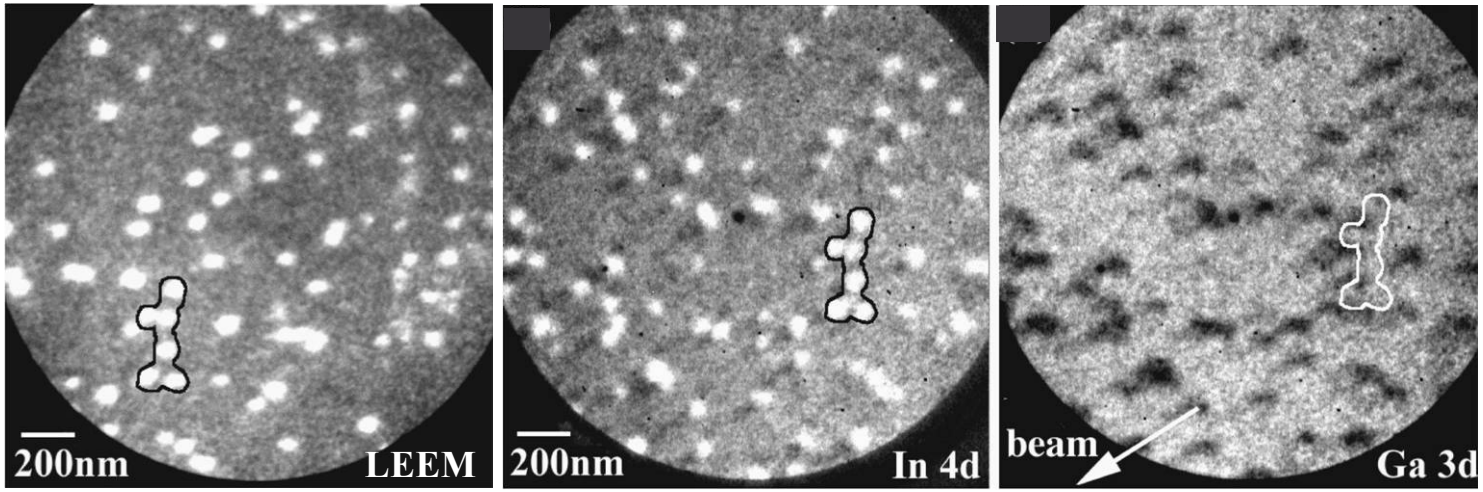


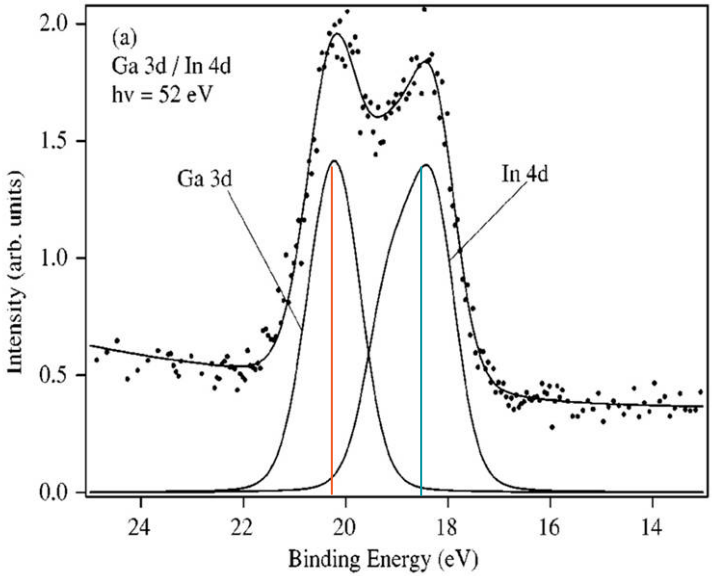


Overall spectra

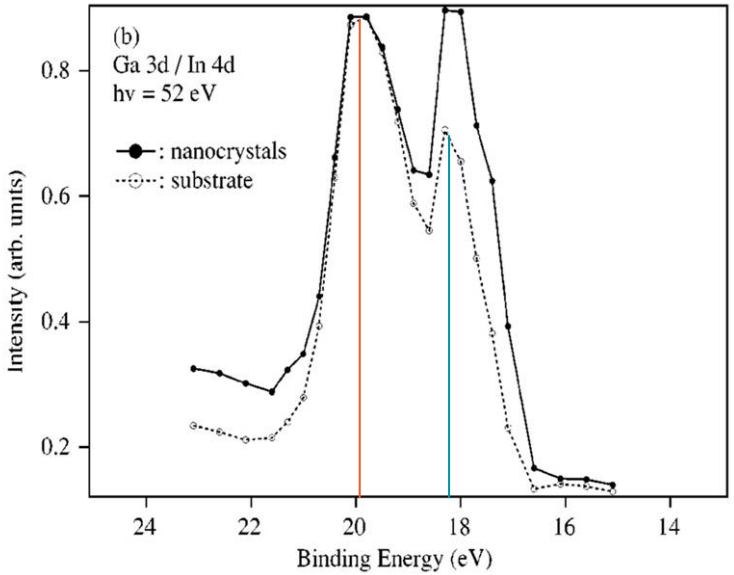


Local spectra

Ga on nanocrystals, In on substrate

intermixing SK growth

S. Heun et al , Phys. Rev B 63 (2001) 125335

# Magnetic imaging

## XMCD, XMLD

# Magnetic imaging in XPEEM

## Ferromagnetism
## Imaging modes

**Sample: 10 Fe monolayers on W (100)**

| | XMCD | | XMCD | XMLD |
|---|---|---|---|---|
| sensitive to | $M_{\parallel}$ | | $M_{\parallel}$ | $M_{\perp}$ |
| | 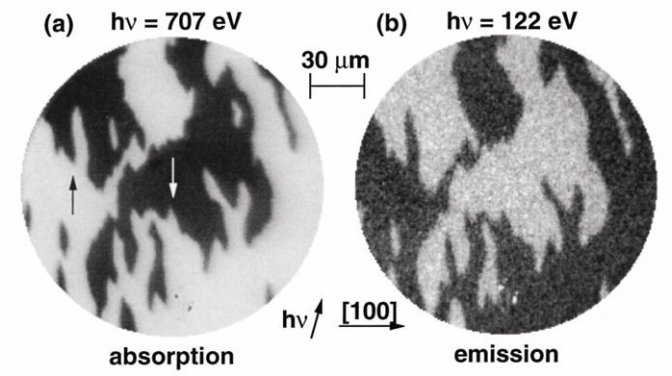 | | 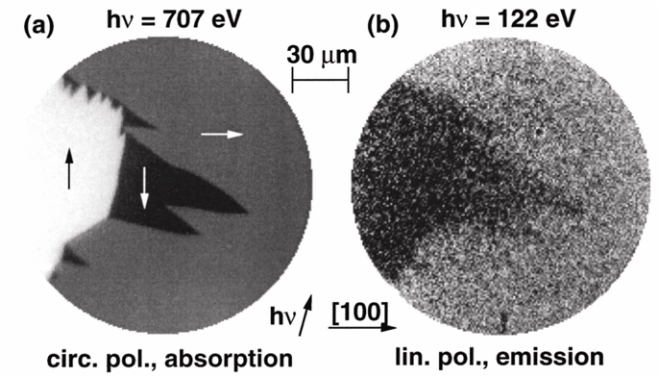 | |
| | secondary electrons from 2p ionization without filter | photo electrons from valence band with high pass filter E > 117 eV | secondary electrons from 2p ionization without filter | photo electrons from 3p level with high pass filter |
| | 3 min/helicity | 11 min/helicity | | |
| gray scale: | 25% asymmetry | 4.7% asymmetry | 25% asymmetry | 25% asymmetry |





asymmetry: XMCD: $(I_{\sigma-}-I_{\sigma+})/(I_{\sigma-}+I_{\sigma+})$ XMLD: $(I_l - I_h)/(I_l + I_h)$

W. Kuch et al, J. Vac. Sci. Technol. B 20 (2002) 2543

# Magnetic imaging with XPEEM

## Antiferromagnetism and ferromagnetism

**NiO (100)**

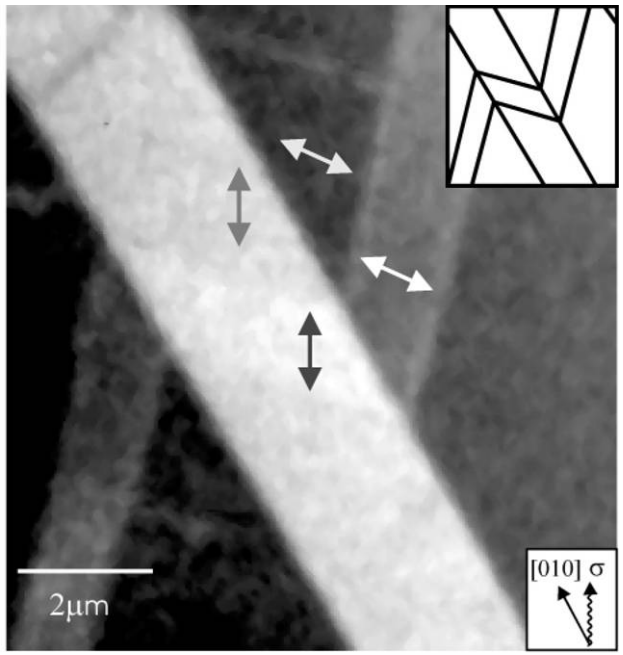


**8 Co monolayers on NiO (100)**

**AF domains**
**Ni $L_2$ images**

**F domains**
**Co $L_3$ images**

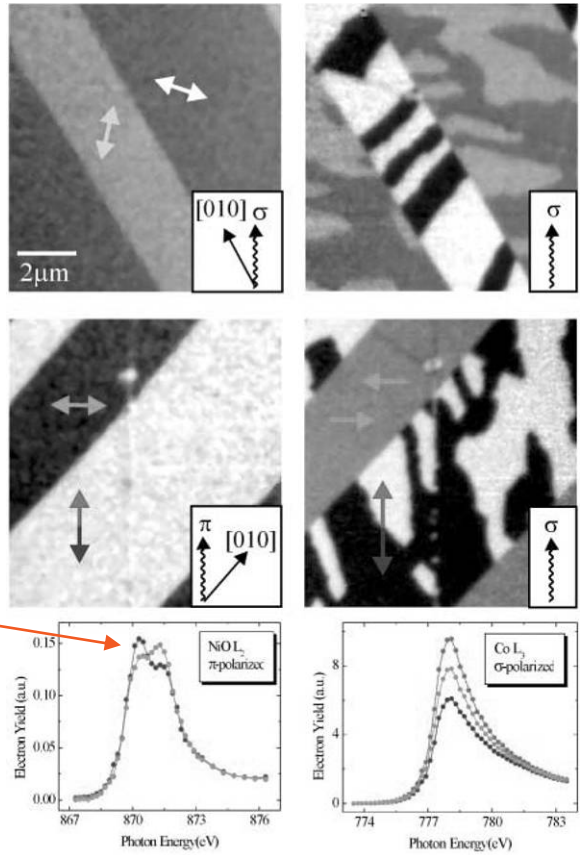


**Contrast from intensity ratio of Ni $L_2$ doublet obtained with circular polarization ($E_\perp/E_\parallel$) σ**
**Arrows: in-plane projections of AF axes obtained with linear polarization ($E_\parallel$) π**

**AF maximum contrast when E ⊥ AF axis**

**Exchange coupling**

H. Ohldag et al, Phys. Rev. Lett. 86 (2001) 2878

# Closure domains in permalloy squares

**Ion beam milled from permalloy film**

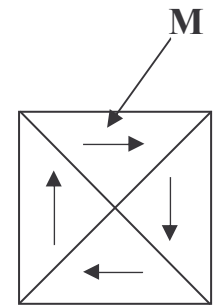


hν

σ

Fe $L_3$ edge

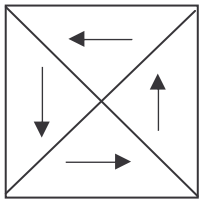

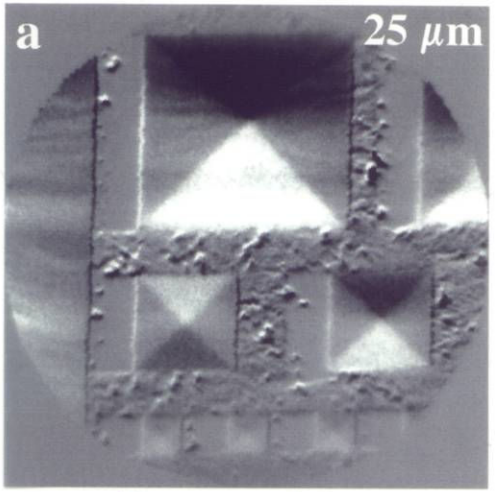


10 μm and 5 μm

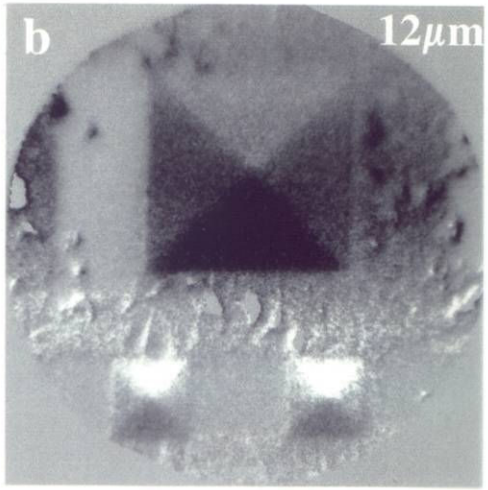


5μm and 2 μm

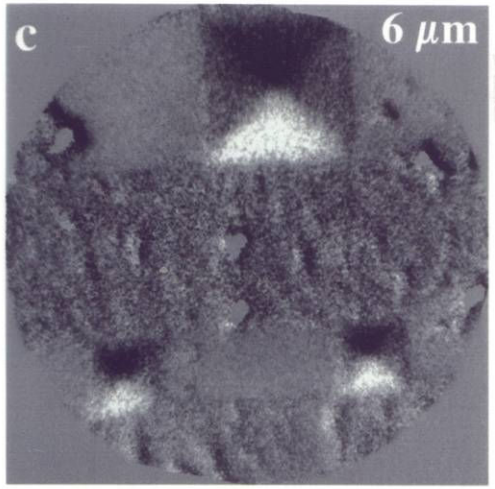


2 μm and 1μm

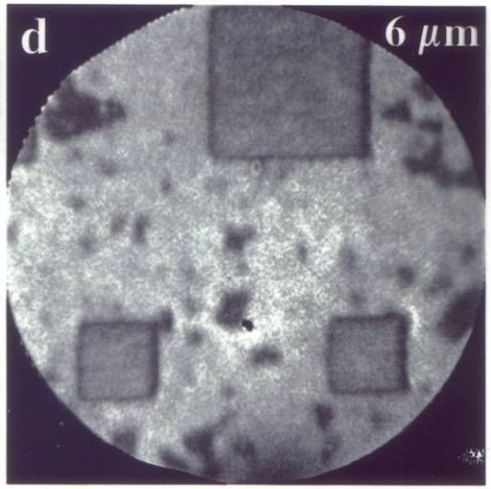


2 μm and 1μm (LEEM)

A. Locatelli et al, Surf. Rev. Lett. 9 (2002) 171

# XMCDPEEM

## Aspect ratio dependence of the virgin domain structure of 1 µm wide Co bits

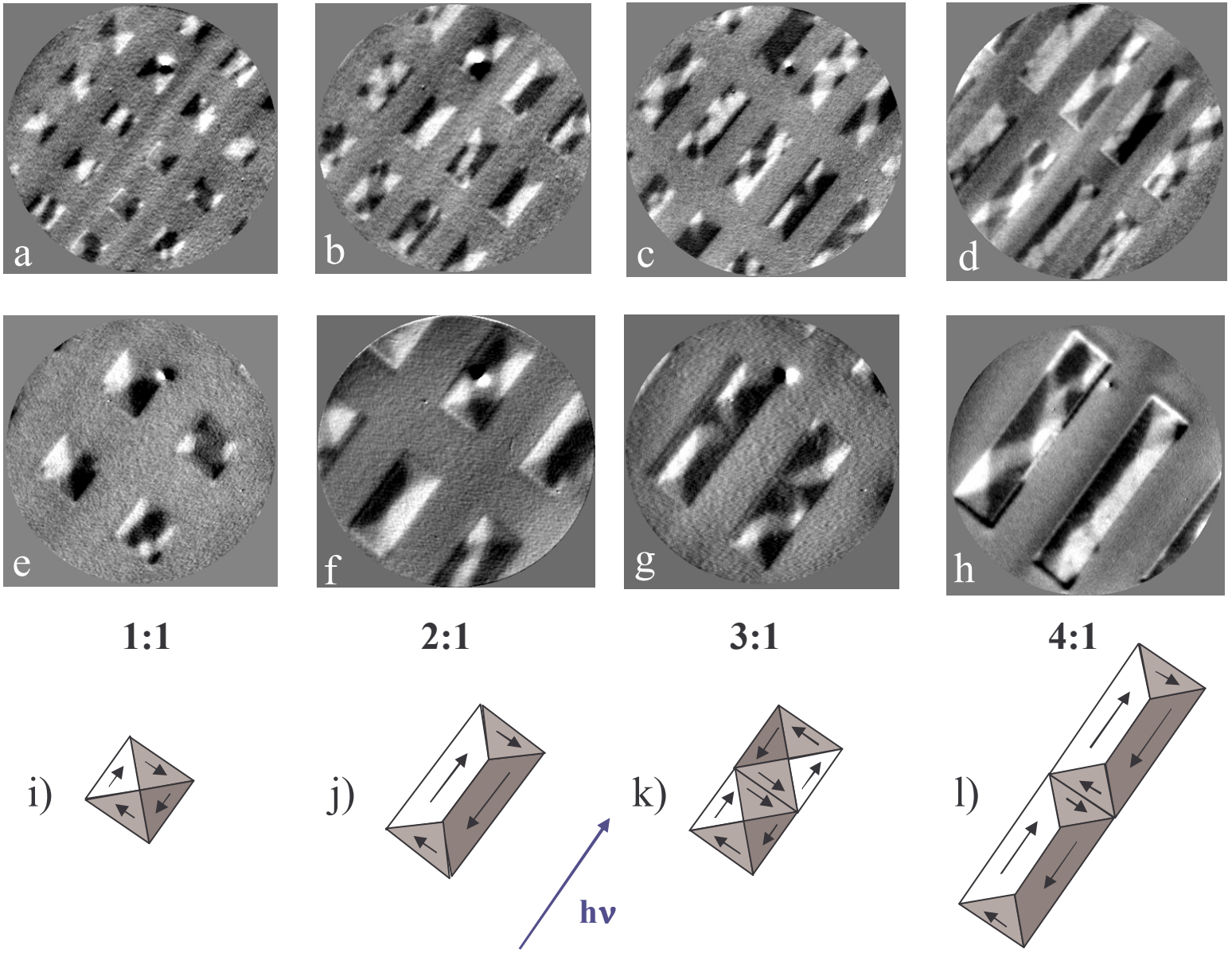

# XMCDPEEM

**Size dependence of the domain structure of 15 nm thick Co bits**
**Aspect ratio 3:1, virgin state**

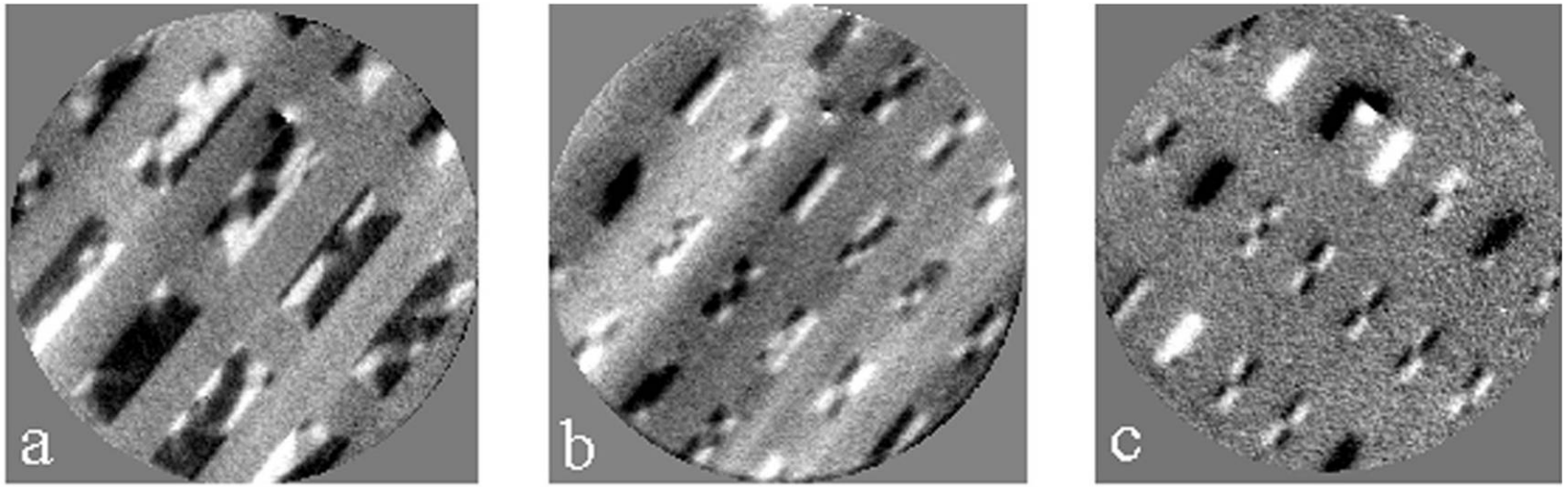


**1000 nm** **500 nm width** **250 nm**

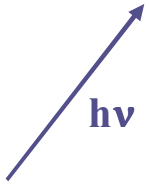

# Micromagnetic simulations of permalloy bits with aspect ratio 2:1

**R. Hertel, Z. Metallk. 93 (2002) 957**

**Landau** **diamond** **S** **C**

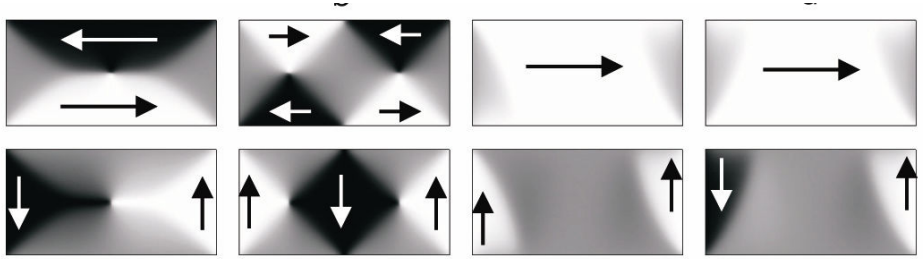

**Size independence**

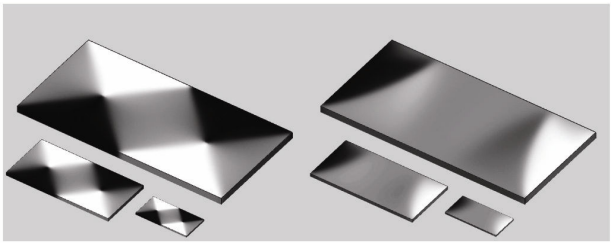

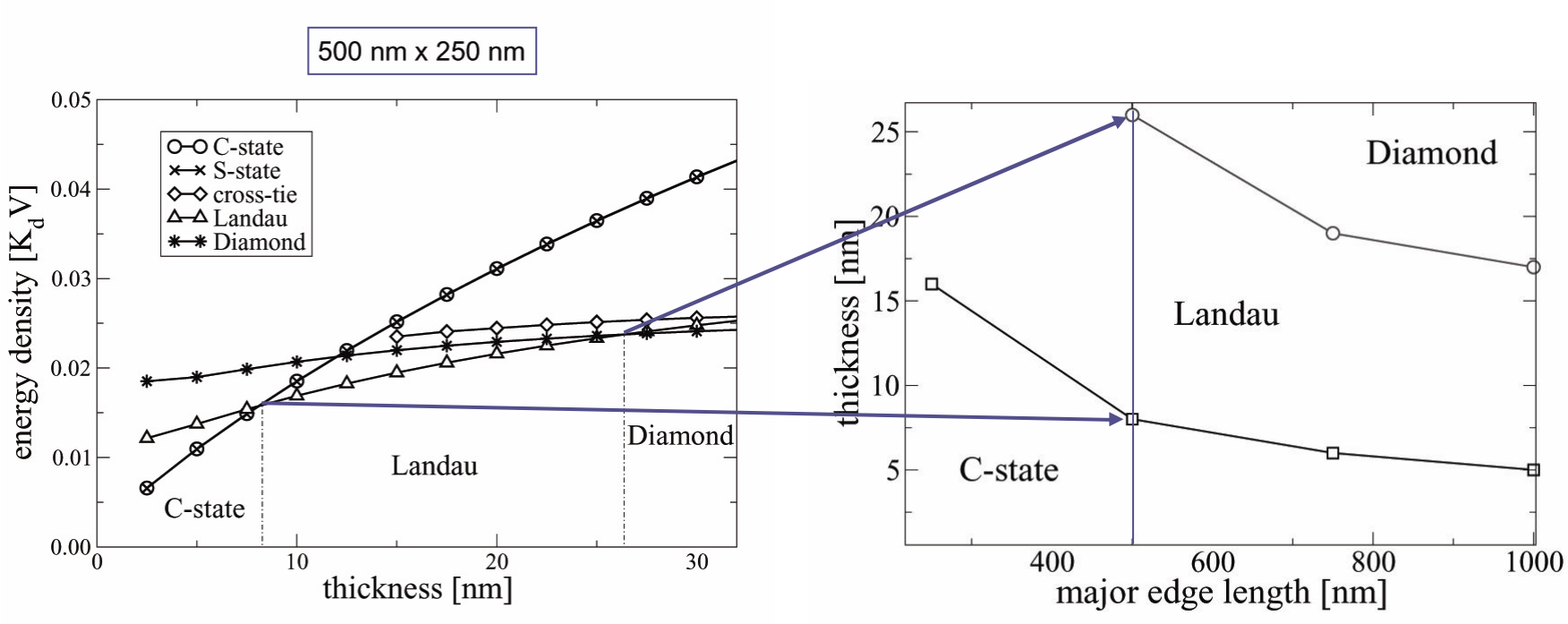

# XMCDPEEM

## Domain structure of 1.6 µm wide Co rings

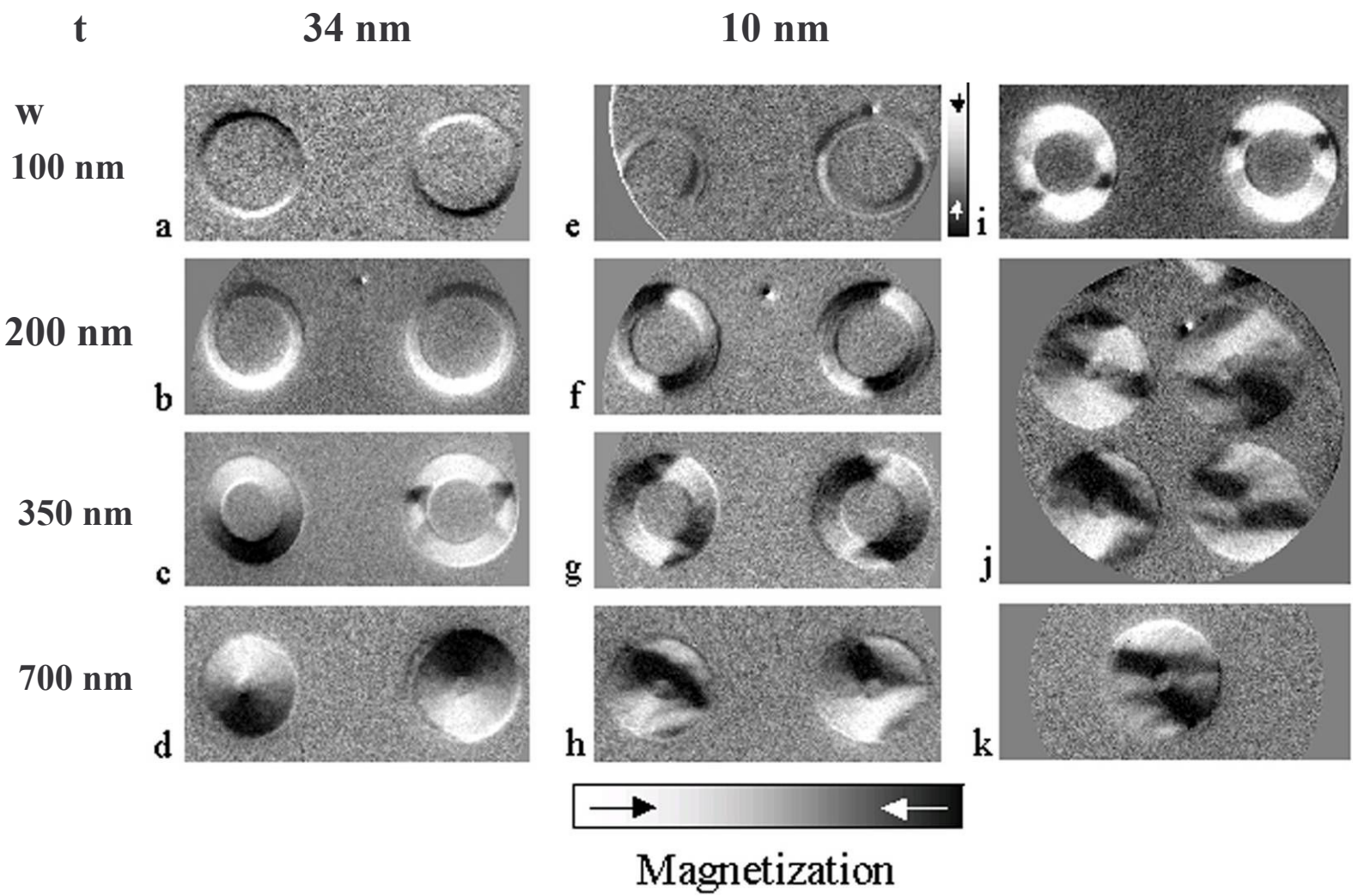

# Micromagnetic simulations of ferromagnetic rings

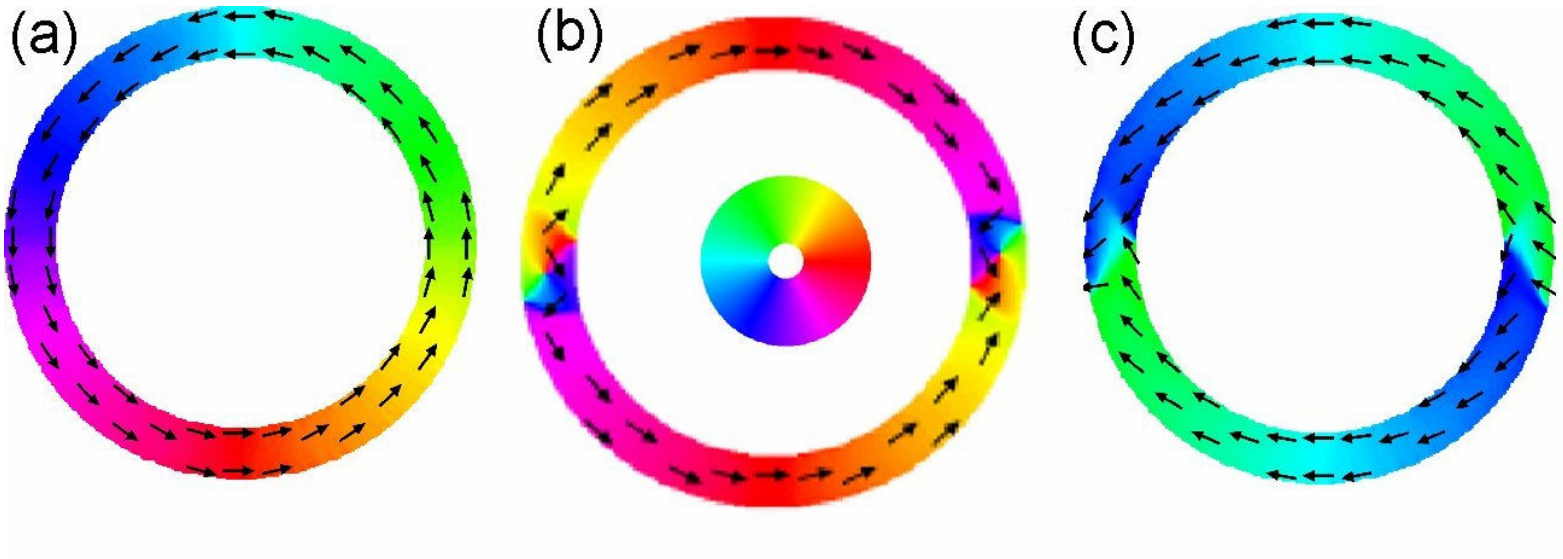


**Vortex state** **Onion states**

**Vortex walls** **Transverse walls**

**M. Kläui, private comm.**

# Onion States

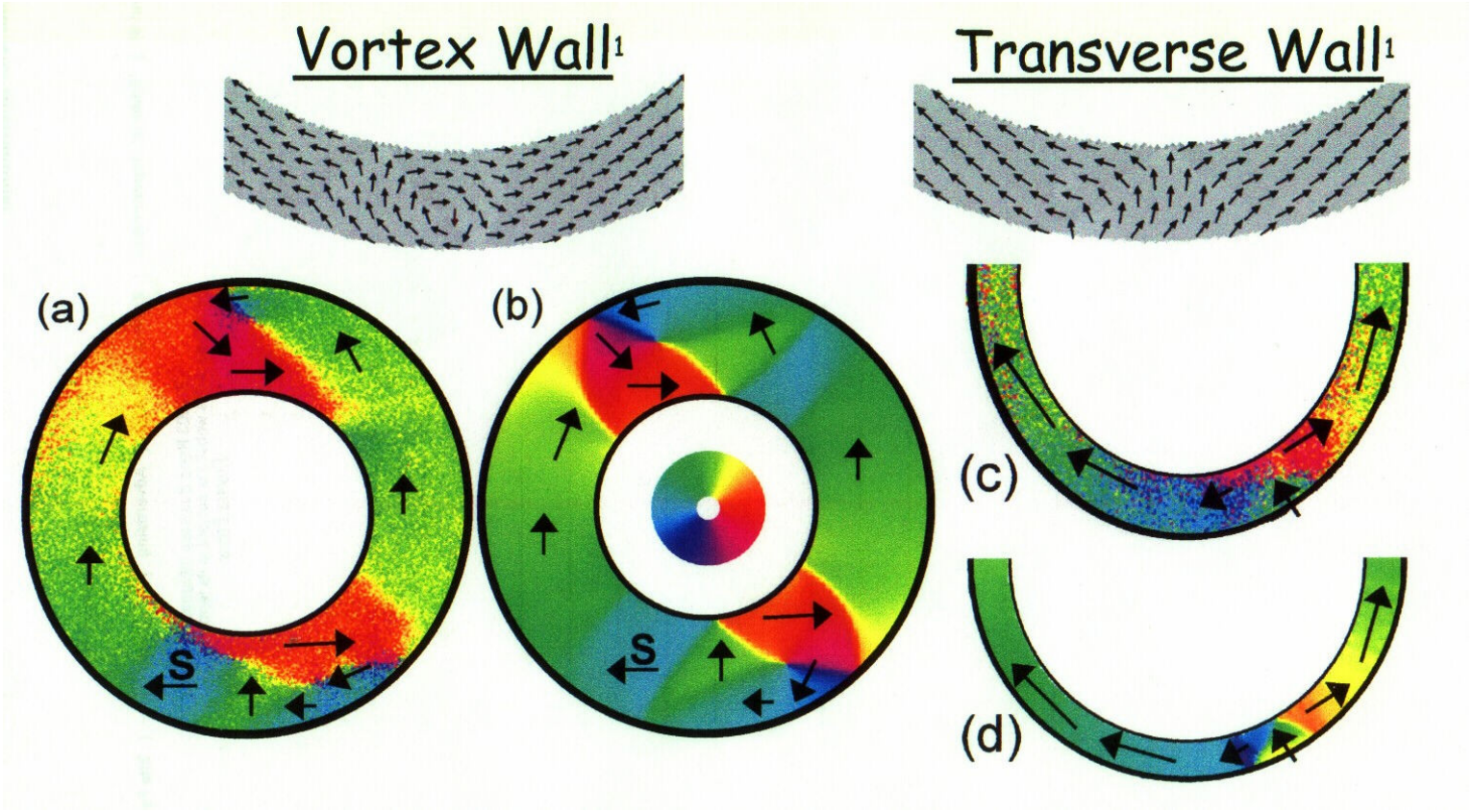


Kläui, priv.commun.

# MnAs

## Bulk properties

### Magnetization

ferromagnetic | paramagnetic

α | β

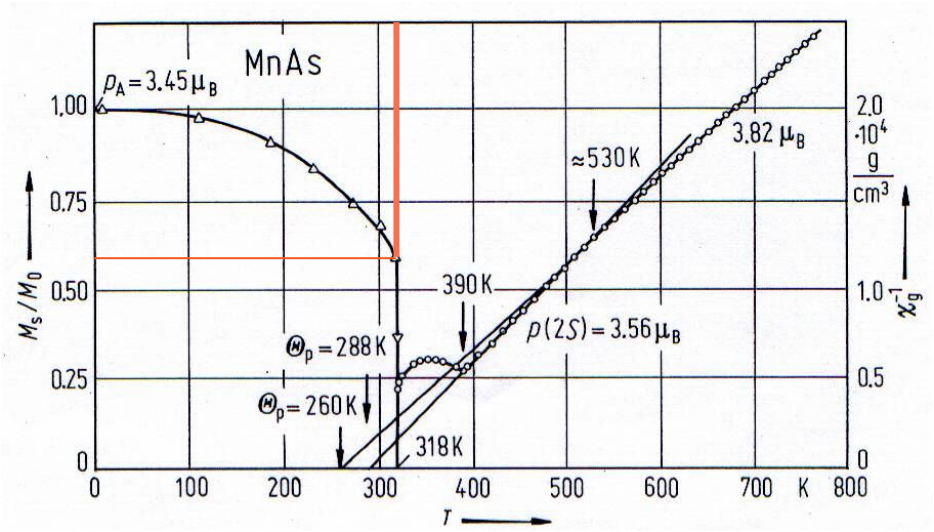


**Sudden loss of magnetization at structural transition**

### Thermal expansion a, c, V

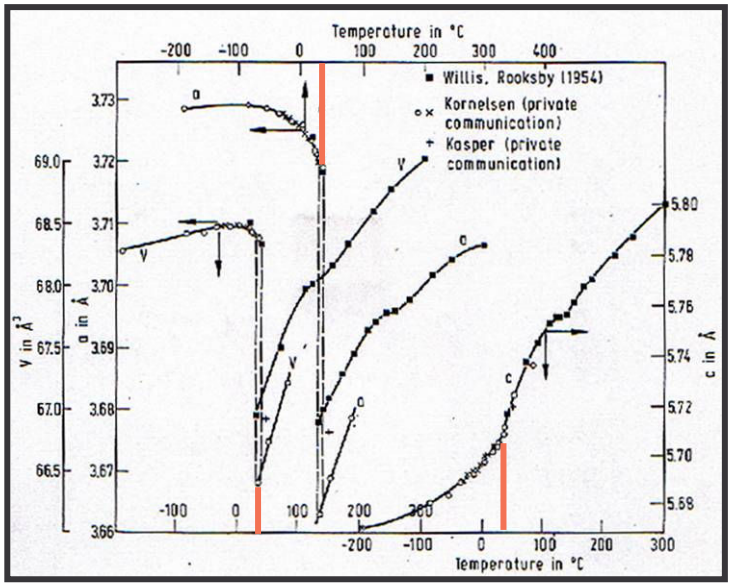


**Large a contraction, little c expansion at phase transition**

**MnAs**

α T< ≈ 40 °C NiAs (hexagonal) ferromagnetic
β MnP (orthorhombic) paramagnetic
γ T > 125 °C NiAs (hexagonal) paramagnetic

## MnAs for spin injection into GaAs at room temperature?

**Problem: strain-induced phase coexistence between ferromagnetic and paramagnetic phase around room temperature**

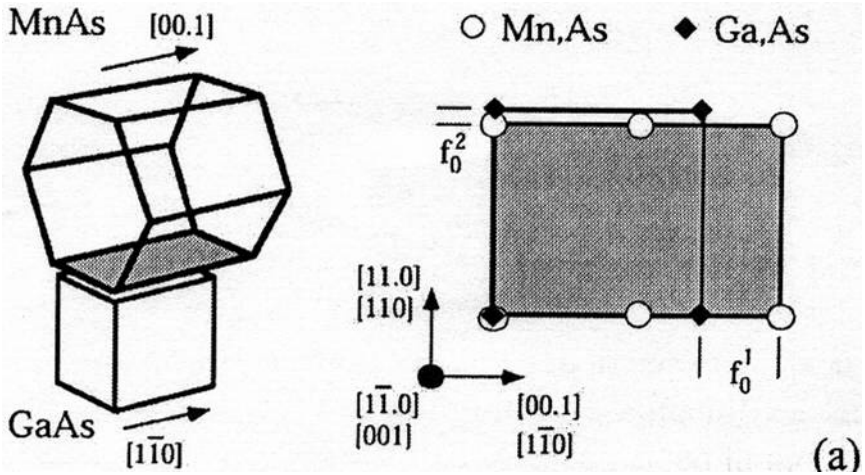


α MnAs / GaAs(100) $f_0^2 = 7.7\%$

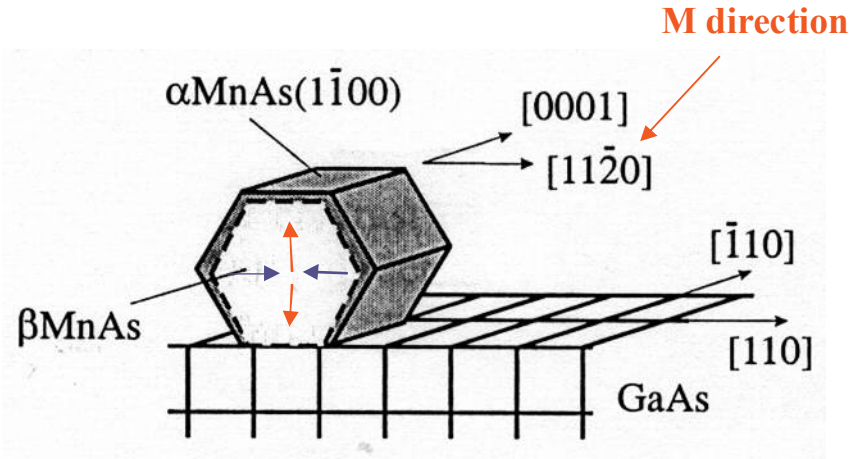


from L. Daeweritz et al ≥ 1999

# Fully magnetized MnAs layer on GaAs (100)

**partially covered with As**
**magnetic contrast formation**

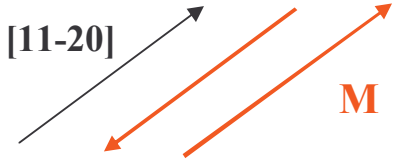


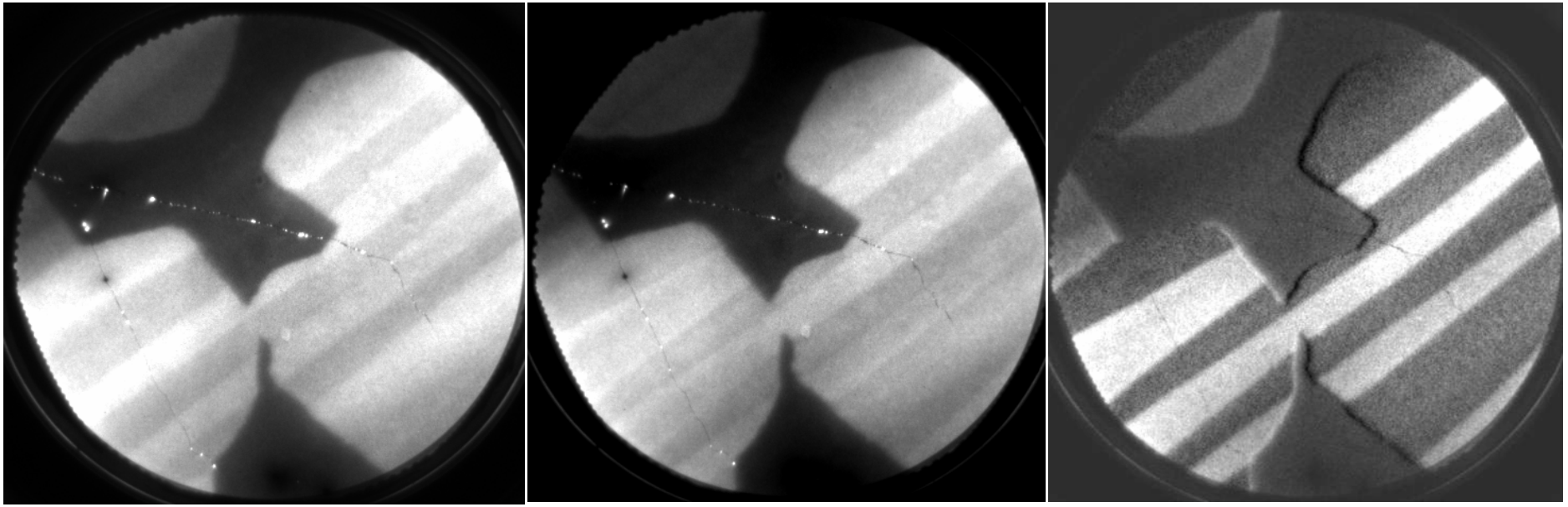

**helicity 1** **helicity 2** **helicity 1 – helicity 2**

**1 µm**

# MnAs islands on GaAs (100)
# far below phase transition
# surrounded by crystallized As capping

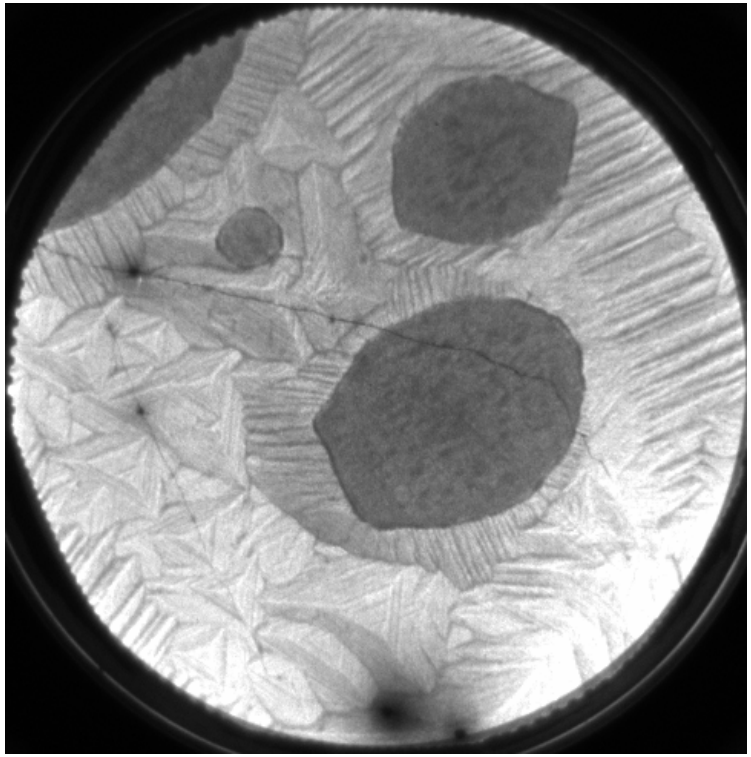

10 eV

1 µm

LEEM

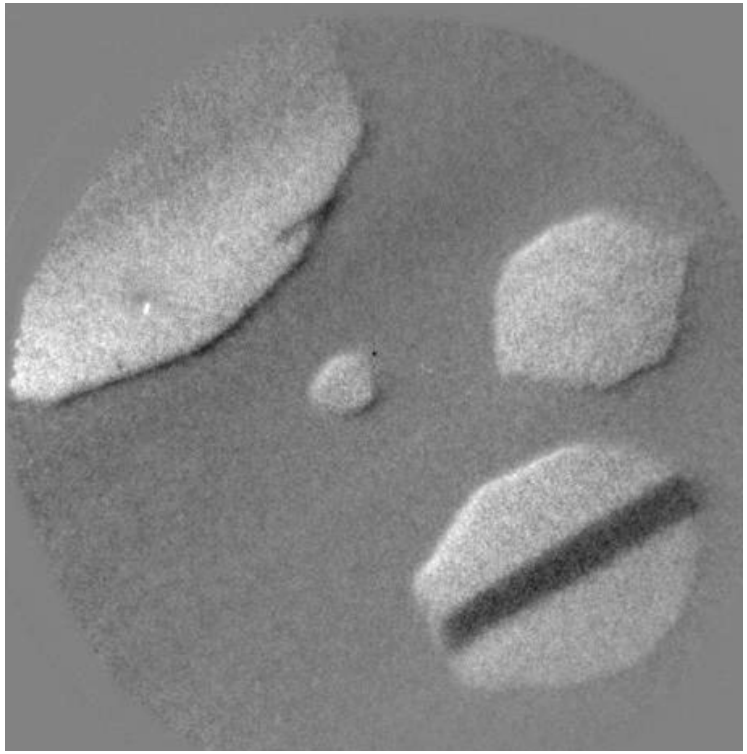

hν = 639.5 eV

XMCDPEEM

# MnAs islands on GaAs(100) in the phase transition region

**Phase contrast**
**between hexagonal and orthorhombic phase**


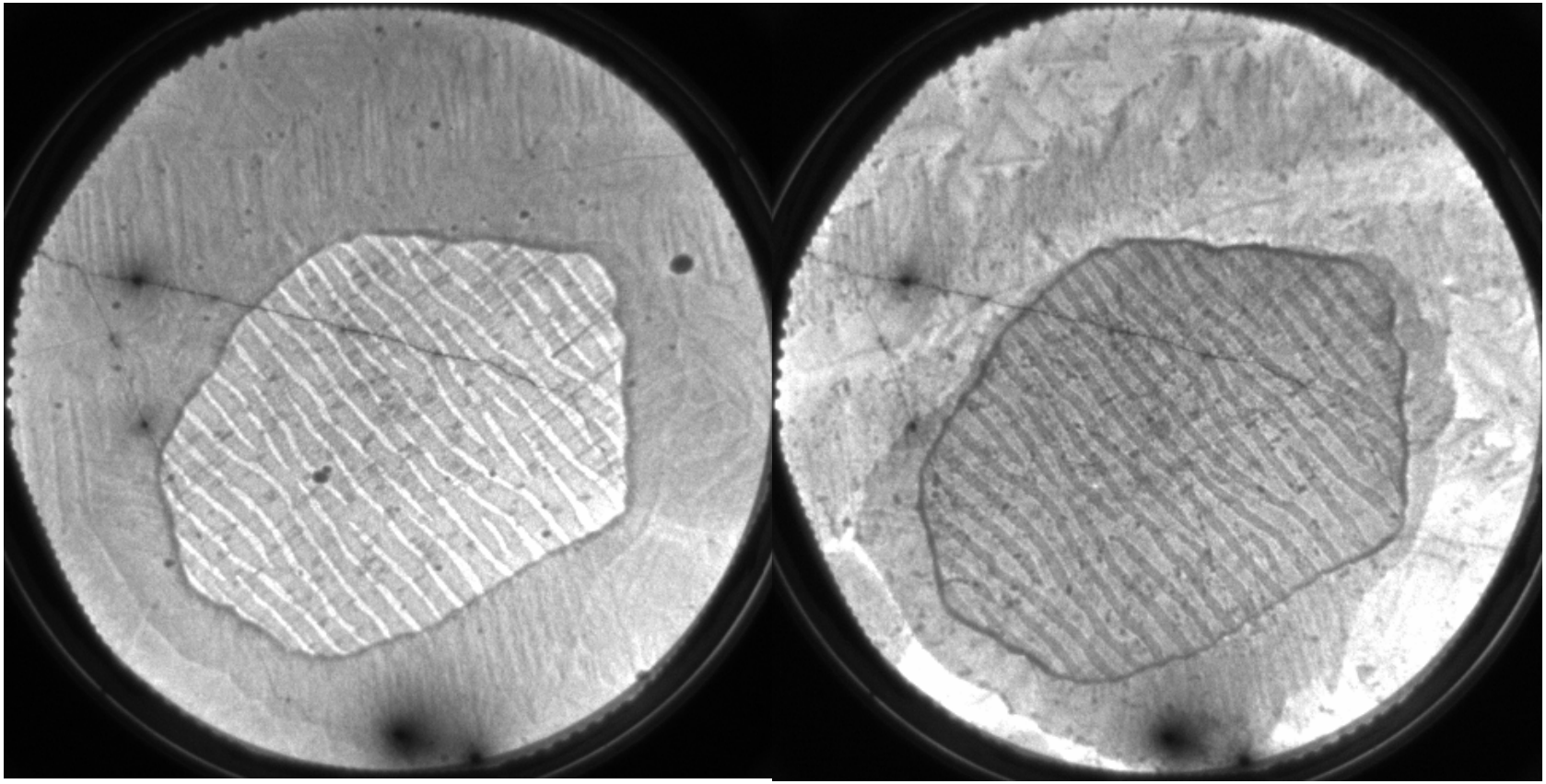

**- 12 µm defocus** **4.5 eV** **+ 12 µm defocus**

**LEEM** **1µm**

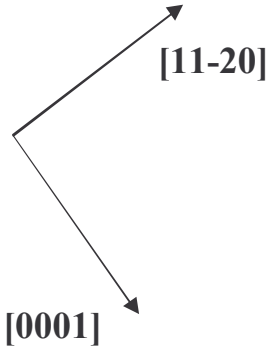


# MnAs / GaAs(100) 40 nm

**XMCDPEEM Mn $2p_{3/2}$ (639.5 eV)**

**during heating**


**during cooling**

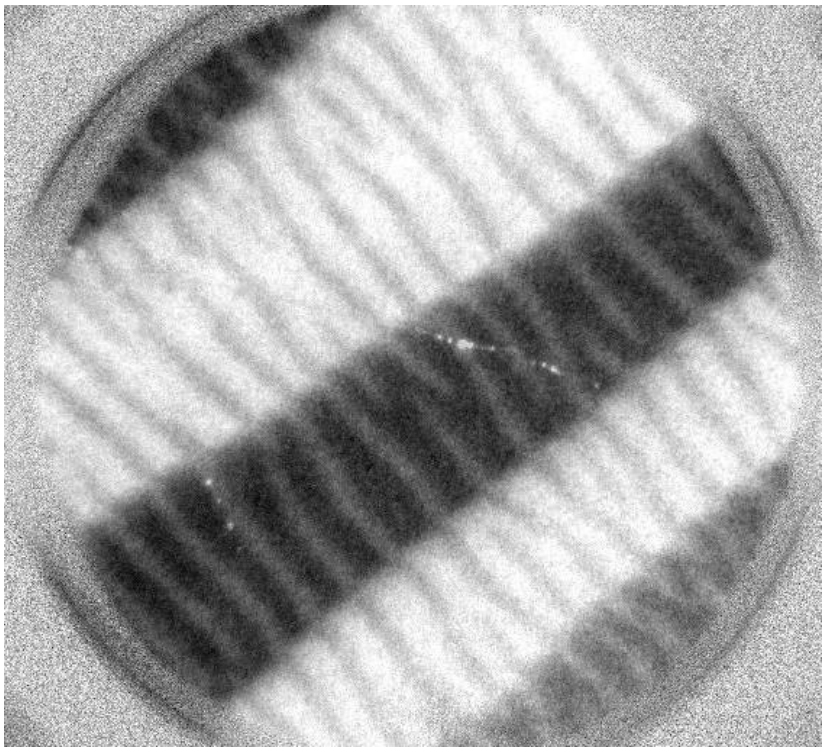

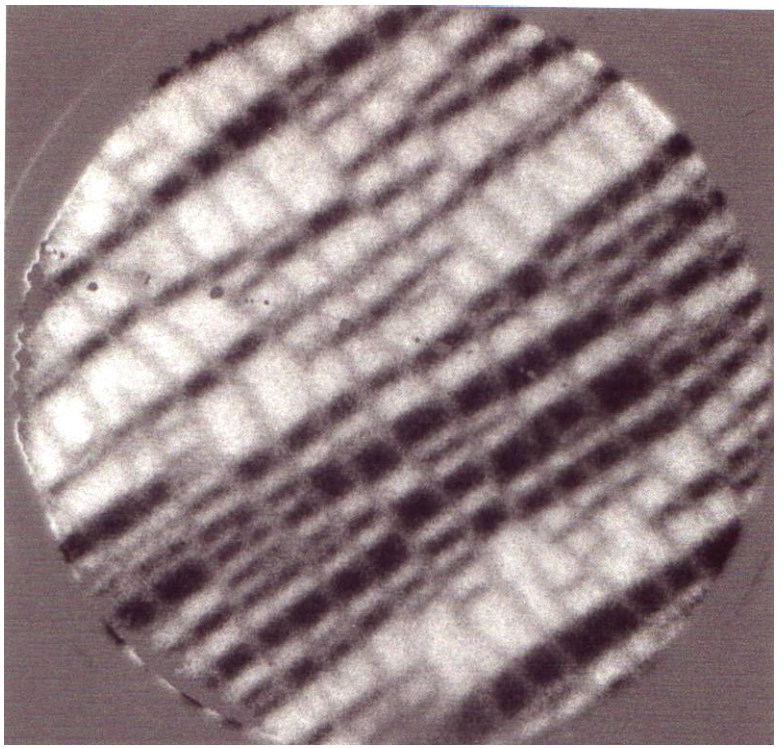

**1 µm**

# Structural - magnetic phase transition in 40 nm thick epitaxial MnAs layer on GaAs (001)

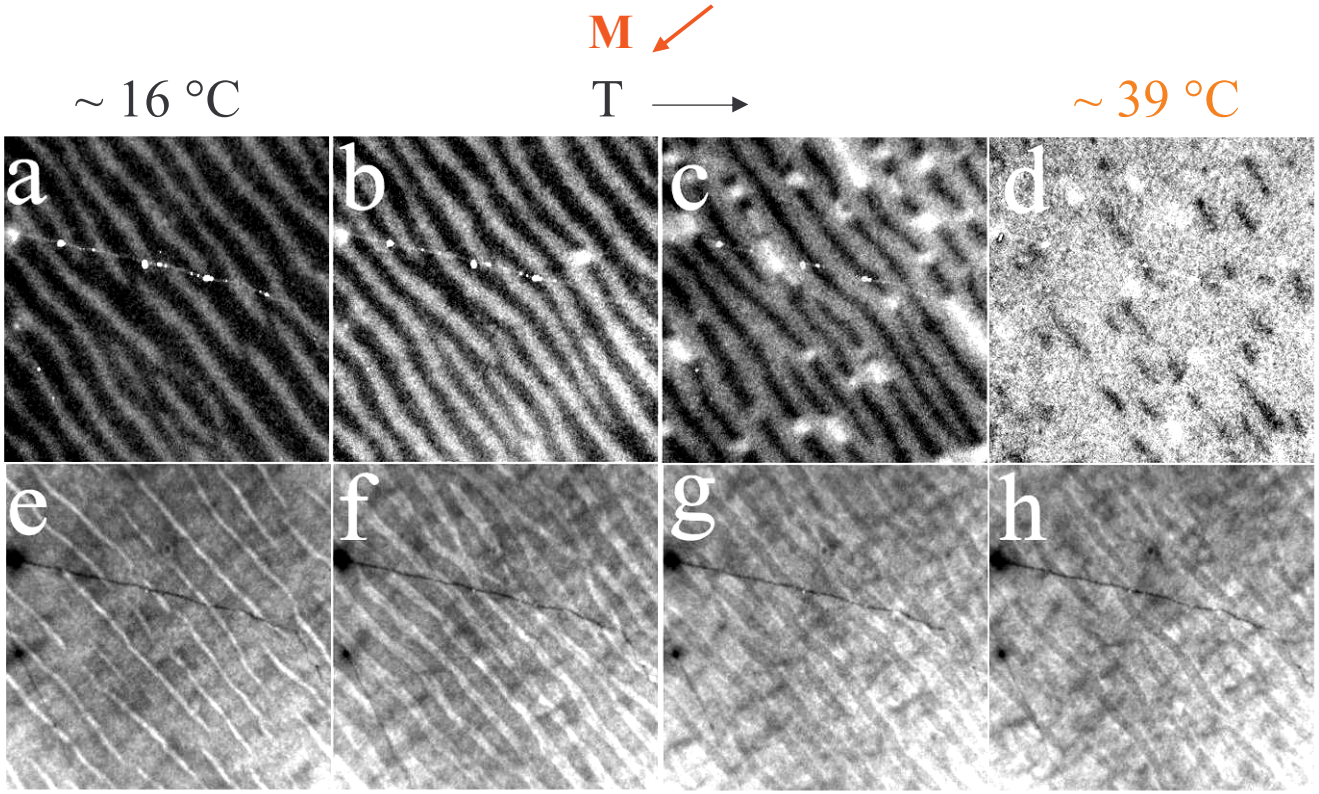


a - d XMCDPEEM
$MnL_3$ (639.5 eV)

1 µm

e - h LEEM
4.5eV

# MnAs / GaAs(100)

**Thickness 40 nm**

**Ferromagnetic – paramagnetic phase transition**

**≈ 13 °C - ≈ 35 °C**

**black M**
**white M**

**gray paramagnetic**

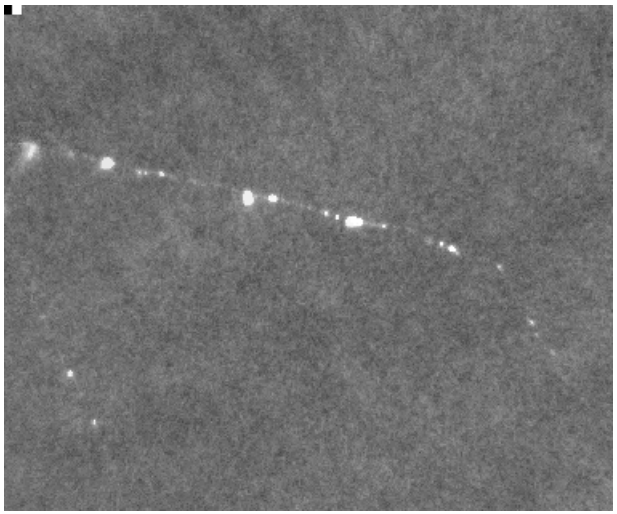

Field of view 4x4 $\mu m^2$

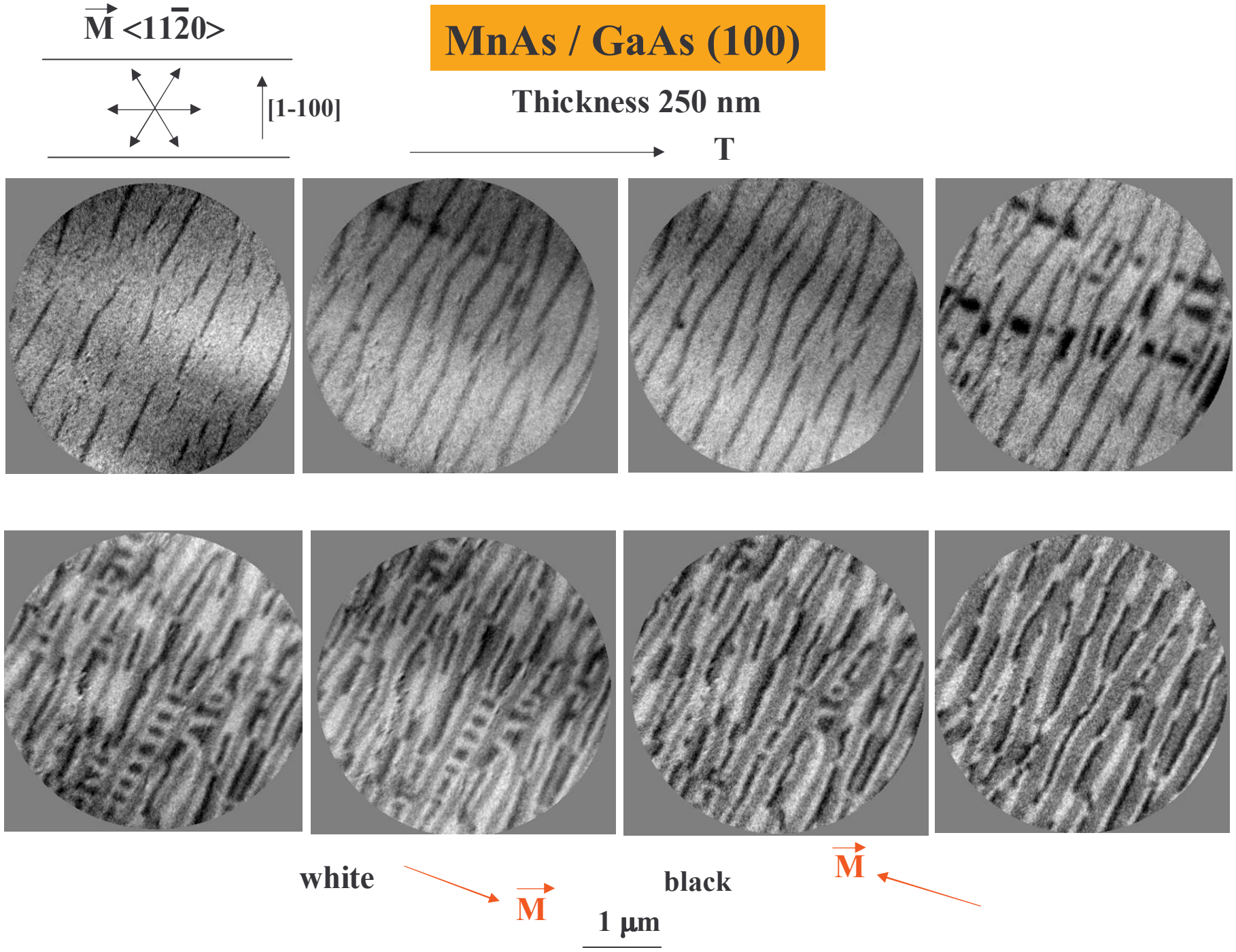
M <11$\bar{2}$0>
[1-100]
MnAs / GaAs (100)
Thickness 250 nm
T
white
M
black
M
1 µm

# MnAs on GaAs(100)

## Thickness dependence of stripe period
## Structural images (LEEM)

**Diameter of field of view**

| 10 μm | 10 μm | 5 μm |
|---|---|---|
| 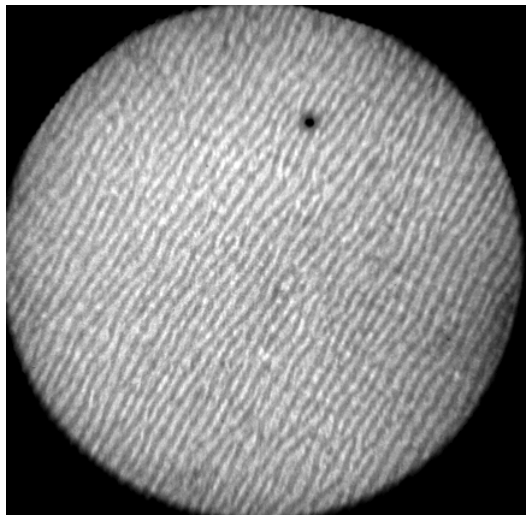 | 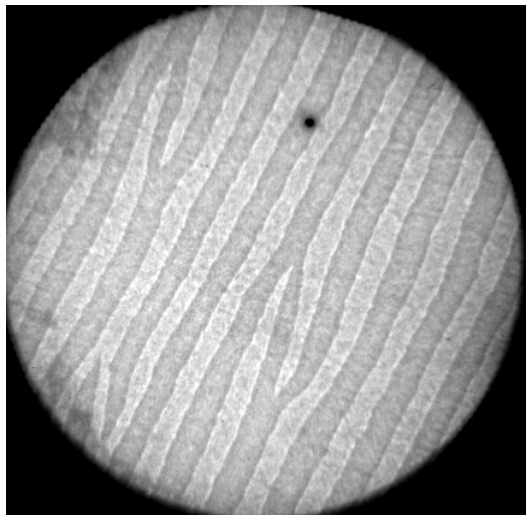 | 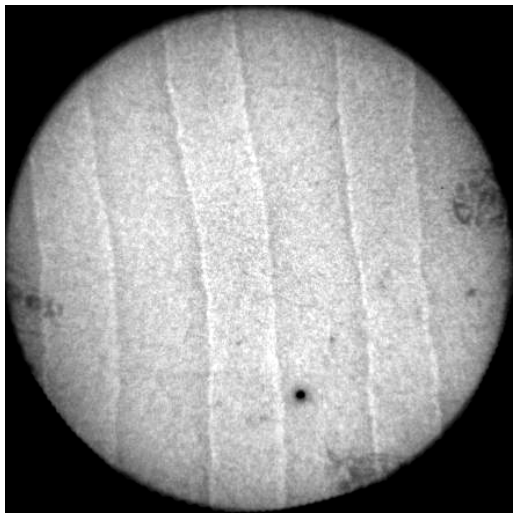 |
| 50 nm | 180 nm | 300 nm |

# MnAs on GaAs(100)

## Thickness dependence of magnetic domain structure

**Room temperature**

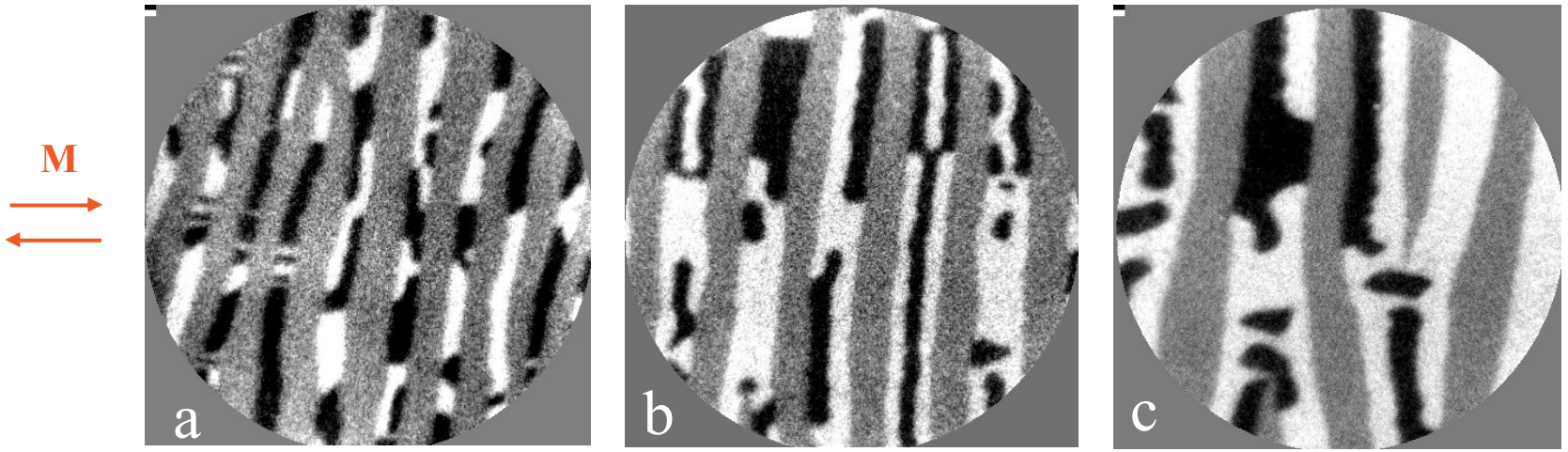


**120 nm** **180 nm** **300 nm**

**Field of view 5 μm diameter**

# MnAs on GaAs(100)

**Thickness 120 nm**
**heating**

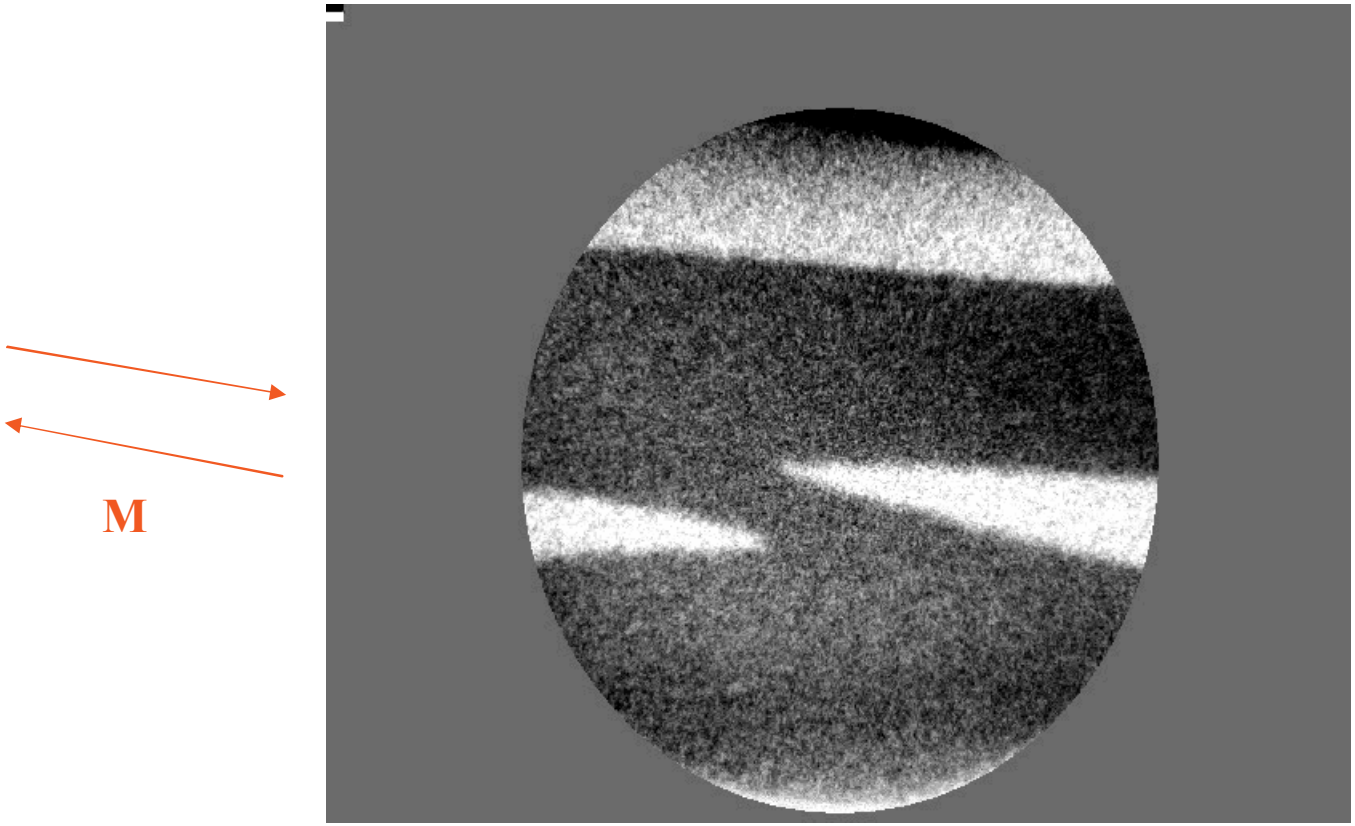


**Field of view 5 μm diameter**

# MnAs on GaAs(100)

**Thickness 180 nm**
**heating**

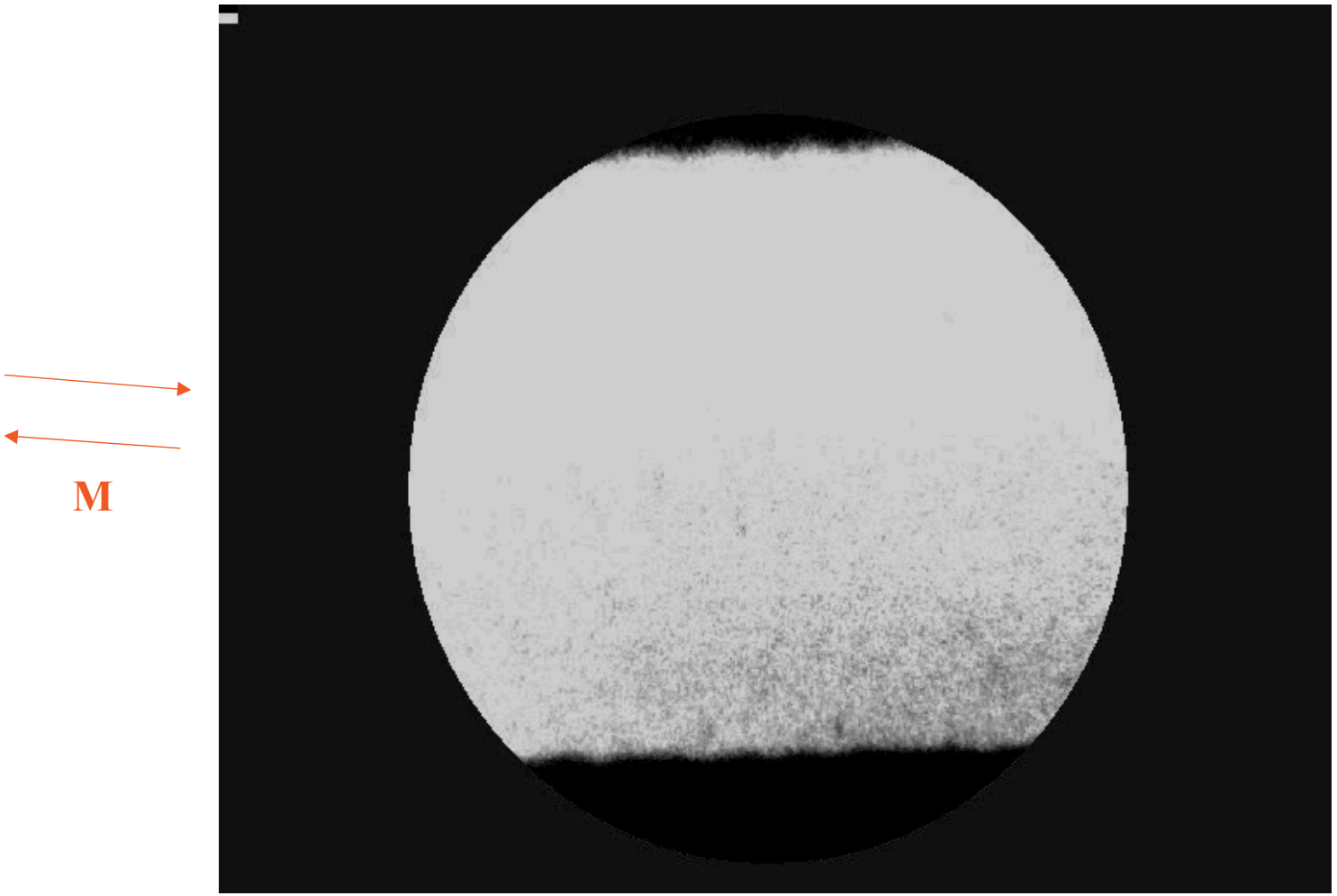


**Field of view 5 μm diameter**

# MnAs on GaAs(311)

**Thickness 180 nm**
**cooling**

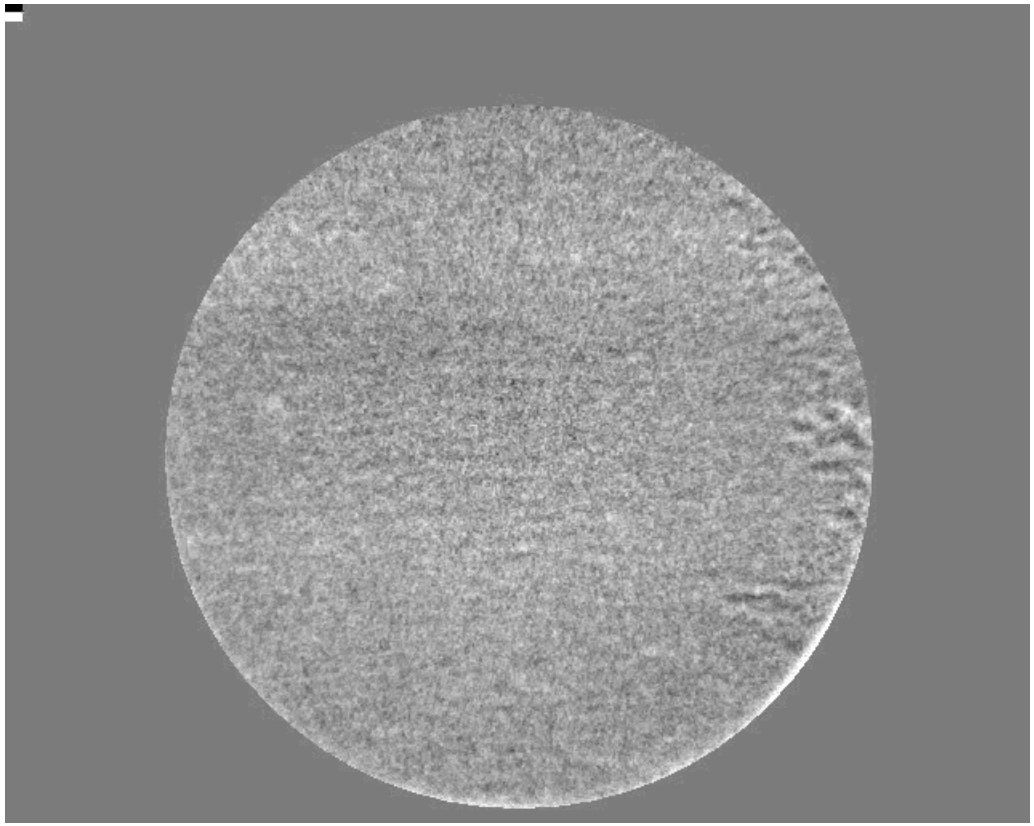

**Field of view 5 μm diameter**

# MnAs on GaAs(100)

**Thickness 300 nm**
**heating**

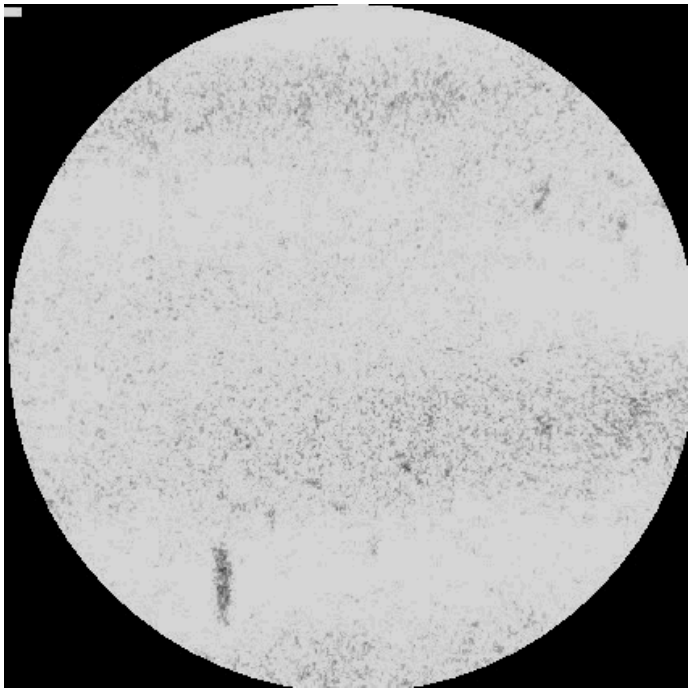

**Field of view 5μm diameter**

# General references


E. Bauer and W. Telieps: *Emission and low energy reflection electron microscopy*, in: Surface and Interface Characterization by Electron Optical Methods, eds. A. Howie and U. Valdre, NATO ASI Series B: Physics, Vol. 191 (Plenum Press, New York 1988) p. 195-233

E. Bauer: *The possibilities for analytical methods in photoemission and low energy electron microscopy*, Ultramicroscopy 36 (1991) 52-62.

E. Bauer, T. Franz, C. Koziol, G. Lilienkamp and T. Schmidt: *Recent Advances in LEEM/PEEM for Structural and Chemical Analysis, in: Chemical, Structural and Electronic Analysis of Heterogeneous Surfaces on Nanometer Scale*, ed. R. Rosei (Kluwer Acad. Publ., Dordrecht 1997) p. 73- 84

E. Bauer, C. Koziol, G. Lilienkamp and T. Schmidt: *Spectromicroscopy in a Low Energy Electron Microscope*, J. Electron Spectrosc. Rel. Phenomena 84 (1997) 201 –209

E. Bauer: *Photoelectron Microscopy*, J. Phys.: Condens. Matter 13 (2001) 11391-11405

E. Bauer: *Photoelectron spectromicroscopy: present and future*, J. Electron Spectrosc.Relat. Phenom. 114 – 116 (2001) 976 –987.

E. Bauer and T. Schmidt: *Multi-Method High Resolution Surface Analysis with Slow Electrons, in: High Resolution Imaging and Spectroscopy of Materials*, ed. by F. Ernst and M. Ruehle (Springer, Berlin Heidelberg 2003) 363-390

Th. Schmidt, U. Groh, R. Fink, E. Umbach, O. Schaff, W. Engel, B. Richter, H. Kuhlenbeck, R. Schloegl, H.-J. Freund, A. M Bradshaw, D. Preikszas, P. Hartel, R. Spehr, H. Rose, G. Lilienkamp, E. Bauer and G. Benner: *XPEEM with energy-filtering: Advantages and first results from the SMART project*, Surf. Rev. Lett. 9 (2002) 223-232